The Composition of Cometary Volatiles

D. Bockelée-Morvan and J. Crovisier
Observatoire de Paris

M. J. Mumma
NASA Goddard Space Flight Center

H. A. Weaver
The Johns Hopkins University Applied Physics Laboratory

The composition of cometary ices provides key information on the chemical and physical properties of the outer solar nebula where comets formed, 4.6 G.y. ago. This chapter summarizes our current knowledge of the volatile composition of cometary nuclei, based on spectroscopic observations and *in situ* measurements of parent molecules and noble gases in cometary comae. The processes that govern the excitation and emission of parent molecules in the radio, infrared (IR), and ultraviolet (UV) wavelength regions are reviewed. The techniques used to convert line or band fluxes into molecular production rates are described. More than two dozen parent molecules have been identified, and we describe how each is investigated. The spatial distribution of some of these molecules has been studied by *in situ* measurements, long-slit IR and UV spectroscopy, and millimeter wave mapping, including interferometry. The spatial distributions of CO, H_2CO, and OCS differ from that expected during direct sublimation from the nucleus, which suggests that these species are produced, at least partly, from extended sources in the coma. Abundance determinations for parent molecules are reviewed, and the evidence for chemical diversity among comets is discussed.

1. INTRODUCTION

Much of the scientific interest in comets stems from their potential role in elucidating the processes responsible for the formation and evolution of the solar system. Comets formed relatively far from the Sun, where ices can condense, and the molecular inventory of those ices is particularly sensitive to the thermochemical and physical conditions of the regions in the solar nebula where material agglomerated into cometary nuclei. An important issue is the extent to which cometary ices inherited the molecular composition of the natal presolar dense cloud vs. the role of subsequent chemistry and processing in the solar nebula (*Irvine et al.,* 2000a; *Ehrenfreund et al.,* 2004; *Lunine and Gautier,* 2004). Though a variety of subtle evolutionary mechanisms operated for cometary nuclei during their long storage in the Oort cloud and Kuiper belt (*Stern,* 2003) and, for short-period comets, during their many passages close to the Sun, the bulk composition of cometary nuclei is still regarded to be in large part pristine, except possibly for the most volatile ices. Thus, observing comets today provides a window through which we can view an earlier time when the planets were forming.

In this chapter, we discuss our current knowledge of the composition of cometary nuclei as derived from observations in cometary comae of molecular species that sublimate directly from the nucleus. In the common cometary terminology, which will be used here, these species are called *parent molecules*, while their photodestruction products are called *daughter* products. Although there have been *in situ* measurements of some parent molecules in the coma of 1P/Halley using mass spectrometers, the majority of results on the parent molecules have been derived from remote spectroscopic observations at ultraviolet (UV), infrared (IR), and radio wavelengths. The past decade has seen remarkable progress in the capabilities at IR and radio wavelengths, in particular, and over two dozen parent cometary molecules have now been detected. Many new identifications were obtained in Comet C/1996 B2 (Hyakutake), which passed within 0.1 AU of Earth in March 1996, and in the exceptionally active Comet C/1995 O1 (Hale-Bopp). We discuss how each of these molecules was identified, how the spectroscopic data are used to derive abundances, and we describe the abundance variations observed among comets.

We also discuss our current knowledge of the noble gas abundances in cometary nuclei, as these are potentially diagnostic of the role played by cometary bombardment on the formation and evolution of planetary atmospheres. Noble gas abundances are also key indicators of the temperature conditions and condensation processes in the outer solar nebula.

The spatial distribution of several molecules has been investigated *in situ*, by IR and UV long-slit spectroscopy, and by radio mapping. We present observational evidence for the presence of extended sources of molecules in the coma. The brightness distribution and velocity shifts of radio emission lines are diagnostic of the outgassing pattern from the nucleus, and recent results obtained by millimeter interferometry are presented.

Isotopic abundances often provide important insights into the evolutionary history of matter, and we discuss the various isotopic data that have been obtained for cometary parent molecules.

For molecules having at least two identical nuclei, the internal energy levels are divided into different spin species (ortho and para in the simplest case), and we discuss how the observed distribution among these spin species may provide information on the formation temperature of cometary nuclei.

2. INVESTIGATION OF PARENT MOLECULES

2.1. Daughter Products

Most of the cometary species observed at optical and UV wavelengths are radicals, atoms, and ions that do not sublimate directly from the nucleus but are instead produced in the coma, usually during the photolysis of the parent molecules, but also by chemical reactions. The discussion of these secondary species in cometary comae is covered in this book by *Feldman et al.* (2004). The only exception is that CO Cameron band emission, some of which is produced in a prompt process following the photodissociation of CO_2, is discussed below.

2.2. Mass Spectrometry

The *Giotto* spacecraft, which flew by 1P/Halley in March 1986, was equipped with two mass spectrometers suitable for composition measurements: the Neutral Mass Spectrometer (NMS) and the Ion Mass Spectrometer (IMS). These two instruments had a mass resolution of 1 amu/q and mass ranges of 12–50 and 1–57 for NMS and IMS, respectively. The Positive Ion Cluster Composition Analyser of the Rème Plasma Analyser also had some capabilities for studying ions in the 12–100 amu/q range. These instruments provided much new information on the molecular and isotopic composition of cometary volatiles, as detailed in section 5 and section 9. However, the analyses of these data were not straightforward, owing to the limited mass resolution and the need for detailed chemical modeling to deduce neutral abundances from the ion mass spectra (see review of *Altwegg et al.,* 1999, and references therein).

2.3. Spectroscopy

Most electronic bands of cometary parent molecules fall in the UV spectral region. As discussed in section 3.1.2, the electronic states of polyatomic molecules usually predissociate, so the absorption of UV sunlight by these species leads to their destruction rather than fluorescence. As a result, the UV study of cometary parent molecules reduces to investigations of diatomic molecules (e.g., CO and S_2) and the atoms present in nuclear ices, specifically noble gases. Since the terrestrial atmosphere blocks UV light from reaching the surface of Earth, cometary UV investigations are generally conducted from space platforms.

Most parent molecules have strong fundamental bands of vibration in the 2.5–5 μm region, where there is abundant solar flux for exciting infrared fluorescence and where thermal radiation and reflected sunlight from dust is not very strong. This near-IR spectral region, which is partly accessible from Earth-based observations, has been a rich source of molecular identifications in cometary comae. The first high-spectral-resolution measurements ($\lambda/\delta\lambda \sim 10^5$–$10^6$) in this region were made during observations of Comet 1P/Halley from the NASA Kuiper Airborne Observatory (KAO) in 1985. The entire region was explored at modest spectral resolution by the Infra Krasnoe Spectrometre (IKS) instrument onboard the *Vega* probe to 1P/Halley ($\lambda/\delta\lambda \sim 50$) and, more recently, by the Infrared Space Observatory (ISO) observations of Comet Hale-Bopp and 103P/Hartley 2 ($\lambda/\delta\lambda \sim 1500$). The advent of sensitive, high-dispersion spectrometers at the NASA Infrared Telescope Facility (IRTF) and Keck telescopes revolutionized this field. Their spectral resolving power (~20,000) allows resolution of the rotational structure of the vibrational bands, which is very important for investigating the internal excitation of the molecules and for unambiguously identifying molecules in the spectrally confused 3.3–3.6 μm region, where the fundamental C–H stretching vibrations lie for all hydrocarbons. Infrared spectroscopy is particularly useful for studying symmetric molecules, which do not have permanent electric dipole moments and thus cannot be observed in the radio range.

Radio spectroscopy is a powerful technique for studying molecules in cold environments via their rotational transitions. This technique has produced many discoveries of cometary parent molecules and is more sensitive than IR and UV spectroscopy for comets observed at large heliocentric distances. With a few exceptions, observations have been made in the 80–460 GHz frequency range from ground-based telescopes. The Submillimeter Wave Astronomy Satellite (SWAS) and the Odin satellite, which observed the 557 GHz H_2O rotational line in several comets, initiated investigations of submillimetric frequencies not observable from Earth. Radio spectrometers provide high spectral resolution ($\lambda/\delta\lambda \sim 10^6$–$10^7$), which permits investigations of gas kinematics through line profile measurements (typical cometary line widths are ~2 km s^{-1}), and which eliminates most ambiguities related to line blending, galactic confusion, or instrumental effects. Most detected molecules were observed in several lines, thereby securing their identification.

3. EXCITATION PROCESSES: LINE/BAND INTENSITIES

3.1. Overview: Main Processes

The interpretation of line or band intensities of parent molecules in terms of column densities and production rates requires the knowledge of the processes that govern their

excitation and emission in the coma. Two kinds of excitation mechanisms can be distinguished: radiative processes and collisional excitation.

3.1.1. Radiative vibrational excitation. For most parent molecules, the main radiative excitation process is radiative excitation of the fundamental bands of vibration by direct solar radiation (*Mumma,* 1982; *Yamamoto,* 1982; *Crovisier and Encrenaz,* 1983; *Weaver and Mumma,* 1984). The pumping rate g_{lu} (s^{-1}) for an individual ro-vibrational transition $l \rightarrow u$ is given by

$$g_{lu} = \frac{c^3}{8\pi h \nu_{ul}^3} \frac{w_u}{w_l} A_{ul} \mathcal{J}(\nu_{ul}) \quad (1)$$

where the lower level l belongs to the v" vibrational state (v" = 0 for fundamental bands), and the upper level u belongs to the excited v' vibrational state. ν_{ul} is the frequency of the transition, w_l and w_u are the statistical weights of the lower and upper levels, respectively, and A_{ul} is the spontaneous emission Einstein coefficient for $u \rightarrow l$. $\mathcal{J}(\nu_{ul})$ is the energy density per unit frequency of the radiation field at the frequency ν_{ul}. The solar radiation in the infrared can be described approximately by a blackbody at T_{bb} = 5770 K and having solid angle Ω_{bb} ($\Omega_{bb}/4\pi = 5.42\ 10^{-6}\ r^{-2}$, where r is the heliocentric distance in AU). Then

$$g_{lu} = \frac{\Omega_{bb}}{4\pi} \frac{w_u}{w_l} A_{ul} (e^{h\nu_{ul}/kT_{bb}} - 1)^{-1} \quad (2)$$

The band excitation rate $g_{v"v'}$, which is the relative number of molecules undergoing vibrational v" → v' excitation through all possible $l \rightarrow u$ transitions within the (v',v") band at frequency $\nu_{v'v"}$, can be approximated by (*Crovisier and Encrenaz,* 1983)

$$g_{v"v'} = \frac{\Omega_{bb}}{4\pi} A_{v'v"} (e^{h\nu_{v'v"}/kT_{bb}} - 1)^{-1} \quad (3)$$

$A_{v'v"}$ is the band spontaneous emission Einstein coefficient, which can be related to the total band strength measured in the laboratory. Practically, the individual spontaneous emission rates A_{ul} required to compute the individual excitation rates g_{lu} (equation 2) can be derived from absorption line intensities measured in the laboratory. The HITRAN (*Rothman et al.,* 2003) and GEISA (*Jacquinet-Husson et al.,* 1999) databases list absorption line intensities and frequencies for ro-vibrational and pure rotational transitions of many molecules. More extensive databases for pure rotational transitions are those of the Jet Propulsion Laboratory (*Pickett et al.,* 1998) and the University of Cologne (*Müller et al.,* 2001). For linear or symmetric-top molecules without electronic angular momentum, simple formulae approximate the A_{ul} and g_{lu} quantities as a function of the total band Einstein coefficient $A_{v'v"}$ and excitation rate $g_{v"v'}$, and the rotational quantum numbers (*Bockelée-Morvan and Crovisier,* 1985). Typically, the strongest fundamental vibrational bands of cometary parent molecules have spontaneous emission Einstein coefficients $A_{v'v"}$ in the range 10–100 s^{-1}, and band excitation rates $g_{v"v'}$ of a few 10^{-4} s^{-1}. Harmonic and combination bands have intrinsic strengths, and thus excitation rates, much smaller than those of the fundamental bands. The pumping from excited vibrational states is also weak. Indeed, their population is negligible with respect to the population of the ground vibrational state. This can be demonstrated easily. If we ignore collisional excitation, which is negligible for vibrational bands as explained in section 3.1.5, and do not consider possible deexcitation of the v' excited state to vibrational states other than the ground state (this corresponds to pure resonant fluorescence), then the population $n_{v'}$ of this v' band at equilibrium between solar pumping and spontaneous decay is

$$n_{v'} = n_{v"} \frac{g_{v"v'}}{A_{v'v"}} \quad (4)$$

where $n_{v"}$ is the population of the ground vibrational state v" = 0. Combining equations (3) and (4), $n_{v'}/n_{v"}$ only depends upon the frequency of the band and heliocentric distance r, and is equal to a few 10^{-6} at 1 AU from the Sun for most bands. It can be also shown that the timescale for equilibration of this excited v' vibrational state is $1/A_{v'v"}$, typically a fraction of second: The total vibrational populations reach radiative equilibrium almost instantly after release of the molecules from the nucleus. For the same reasons (low populations and small radiative lifetimes), steady-state is achieved locally for the rotational levels within the vibrational excited states. As will be discussed later, this is generally not the case for the rotational levels in the ground vibrational state.

Besides the direct solar radiation field, the vibrational bands can be radiatively excited by radiation from the nucleus and the dust due to scattering of solar radiation or their own emission in the thermal infrared. *Crovisier and Encrenaz* (1983) showed that all these processes are negligible, except excitation due to dust thermal emission, which can be important in the inner comae of active comets for vibrational bands at long wavelengths (>6.7 μm).

3.1.2. Radiative electronic excitation. The electronic bands of diatomic and polyatomic molecules fall in the UV range. Owing to the weak solar flux at these wavelengths, the excitation rates of electronic bands are small compared to vibrational excitation rates. For example, the total excitation rate of the $A^1\Pi$ state of CO by the absorption of solar photons near 1500 Å, which leads to resonance fluorescence in the CO $A^1\Pi$–$X^1\Sigma^+$ Fourth Positive Group, is ~$1–2 \times 10^{-6}$ s^{-1} at r = 1 AU (*Tozzi et al.,* 1998). The latter is roughly two orders of magnitude smaller than the excitation rate by solar radiation of the CO v(1–0) band at 4.7 μm [2.6×10^{-4} s^{-1} at 1 AU (*Crovisier and Le Bourlot,* 1983)]. Therefore, the populations of the ground state rotational levels are not significantly affected by electronic excitation. In addition, electronic bands of polyatomic molecules are often dissociative or predissociative, and their excitation by the Sun generally

only produces weak UV fluorescence. This explains why cometary parent molecules are rarely identified from their electronic bands in UV spectra. The resonance transitions of neutral atoms, including the noble gases that may be present in the nucleus, are at UV and far UV (FUV) wavelengths, but the excitation rates are relatively small because of the low solar flux in these regions. The electronic excitation of CO and S_2, as observed in UV cometary spectra, is reviewed in section 3.4. The computation of electronic excitation rates does not differ much in principle from that of vibrational excitation rates. However, in the UV range the solar spectrum shows strong and narrow Fraunhofer absorption lines, and cannot be approximated by a blackbody. This fine structure results in absorption probabilities that depend on the comet's heliocentric radial velocity, as first pointed out by *Swings* (1941) for the CN radical. This so-called *Swings effect* can introduce large variations in the fluorescence emission spectrum of electronic bands.

3.1.3. Radiative rotational excitation and radiation trapping. Pure rotational excitation by sunlight is negligible because of the weakness of the solar flux at the wavelengths of the rotational transitions. However, at r > 3 AU, rotational excitation by the 2.7 K cosmic background radiation competes with vibrational excitation (which varies according to r^{-2}), and must be taken into account in fluorescence calculations (*Biver et al.,* 1999a).

In the specific case of the H_2O molecule, the rotational excitation is strongly affected by self-absorption effects. Owing to large H_2O densities in the coma, many rotational H_2O lines are optically thick and trap line photons emitted by nearby H_2O molecules. This was modeled by *Bockelée-Morvan* (1987) in the local approximation, using an escape probability formalism. The net effect of radiation trapping is to delay the radiative decay of the rotational levels to the lower states and to maintain local thermal equilibrium at a lower density than would have been required in optically thin conditions (*Weaver and Mumma,* 1984; *Bockelée-Morvan,* 1987). The lower rotational states of H_2O are affected by this process up to distances of a few 10^4 km when the H_2O production rate $Q(H_2O)$ is ~10^{29} molecules s^{-1}.

3.1.4. Fluorescence equilibrium. When the excitation is determined solely by the balance between solar pumping and subsequent spontaneous decay, this establishes a condition called *fluorescence equilibrium.* For the rotational levels within the ground vibrational state, fluorescence equilibrium is reached in the outer, collisionless coma. For molecules with large dipole moments (μ) and large rotational constants, such as H_2O (μ = 1.86 D) or HCN (μ = 2.99 D), infrared excitation rates are generally small compared to the vibrational and rotational Einstein A-coefficients, so that most of the molecules relax to the lowest rotational levels of the ground vibrational state (Fig. 1). Heavy molecules with small dipole moment (e.g., CO with μ = 0.11 D) and symmetric species will have, in contrast, a warm rotational distribution at fluorescence equilibrium. The rotational population distribution gets colder as the comet moves far from the Sun because vibrational excitation becomes less efficient. The timescale for rotational equilibration, which is mainly controlled by pure rotational relaxation for molecules having a nonzero electric dipole moment (vibrational relaxation is more rapid), exceeds 10^4 s for most detected molecules. Some molecules never reach equilibrium during their lifetime.

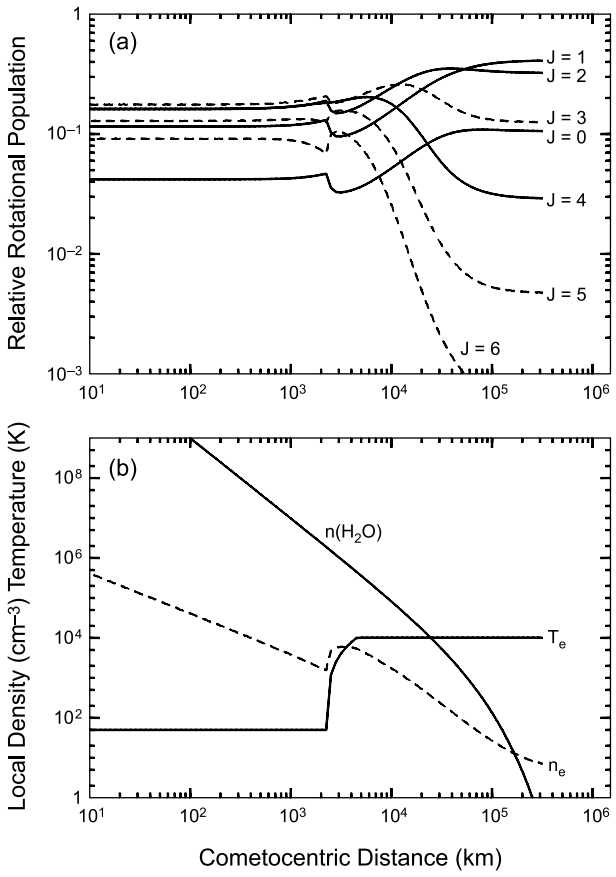

Fig. 1. **(a)** Rotational population distribution of HCN as a function of distance to nucleus for a comet at 1 AU from the Sun with $Q(H_2O) = 10^{29}$ molecules s^{-1} (from the model of *Biver et al.,* 1999a). **(b)** H_2O local density $n(H_2O)$, electronic density n_e and temperature T_e in the model. The gas kinetic temperature is 50 K throughout the coma. The population distribution evolves from thermal equilibrium in the inner coma, to fluorescence equilibrium in the outer coma. The discontinuities at 2×10^3 km are due to the sharp rise of the electron temperature, from 50 to 10,000 K.

3.1.5. Collisional excitation. Collisions, generally involving H_2O molecules and/or electrons, are important in determining the rotational excitation of molecules in the inner coma. For comets at large heliocentric distances, where the CO production rate is much larger than the H_2O production rate, collisional excitation is provided by CO. Collisions with ions are generally considered to be unimportant for parent molecules, but this question has not yet been properly addressed.

Owing to the low temperatures throughout the inner coma [10–100 K (cf. *Combi et al.,* 2004)], collisions do not signi-

ficantly populate either the vibrational or electronic levels of molecules, and the steady-state vibrational and electronic population distributions are determined by radiative processes. Collisions can quench the fluorescence of vibrational bands, but this is generally unimportant, except possibly within a few kilometers of the surface of the nucleus (*Crovisier and Encrenaz,* 1983; *Weaver and Mumma,* 1984).

Collisions thermalize the rotational population of the ground vibrational state at the kinetic temperature of the gas. The collision rate C (s^{-1}) is given by

$$C = \sigma_c n(r_c)\bar{v} \quad (5)$$

where σ_c is the collision cross-section, $n(r_c)$ is the local density of the collision partner at the cometocentric distance r_c, and $\bar{v}$ is the relative speed of the impinging species. To treat collisional excitation properly, we must understand how collisions connect individual rotational states, that is, specify the collision cross-sections σ_{ij} for each $i \rightarrow j$ transition. However, there is little experimental or theoretical information on collisional processes involving neutral molecules (H_2O or CO). Not only are the line-by-line cross-sections not available, but the total cross-sections for collisional deexcitation, which could, in principle, be derived from laboratory measurements of line broadening, are poorly documented for most cometary species. In current cometary excitation models, total cross-sections of ~1–5 $\times 10^{-14}$ cm^2 are assumed (e.g., *Chin and Weaver,* 1984; *Bockelée-Morvan,* 1987; *Crovisier,* 1987; *Biver et al.,* 1999a), based on the broadening of CO and H_2O lines by collisions with H_2O. *Chin and Weaver* (1984) introduced a ΔJ dependence on the rotational CO–H_2O cross-sections and pointed out that collisional excitation of CO is rather insensitive to this dependence as long as the total cross-section is fixed.

The role of electron collisions in controlling rotational populations was first investigated in detail by *Xie and Mumma* (1992) for the H_2O molecule. This study was motivated by the need for large cross-sections to interpret the relative line intensities of the ν_3 H_2O band in Comet 1P/Halley observed preperihelion with the KAO. It was previously recognized that, in the inner coma, inelastic collisions with H_2O would cool hot electrons to the temperature of the gas, transferring their translational energy into rotational H_2O excitation (*Ashihara,* 1975; *Cravens and Korosmezey,* 1986). Unlike neutral-neutral collisions, theoretical determinations of rotational cross-sections are available for collisions involving electrons. Relatively simple formulae were obtained using the Born approximation by Itikawa (1972), which show that cross-sections are directly proportional to the rotational A_{ul} of the transitions and are also a function of the kinetic energy of the colliding electrons. Cross-sections are large for molecules with large dipole moments ($A_{ul} \propto \mu^2$), typically exceeding those for neutral-neutral collisions by two or three orders of magnitude for electrons thermalized at 50 K. Using the electron temperature and density profile measured *in situ* by *Giotto*, *Xie and Mumma* (1992) showed that, for a Halley-type comet, the molecular excitation by e^-–H_2O collisions exceeds that by H_2O–H_2O collisions at cometocentric distances ≥3000 km from the nucleus. Neutral H_2O collisions dominate in the inner coma because the $n(H_2O)/n(e^-)$ local density ratio is very large (Fig. 1). Observational evidence for the important role played by collisions with electrons is now abundant [e.g., *Biver et al.* (1999a) for the excitation of HCN]. So far, the modeling of this process is subject to large uncertainties, as the electron density and temperature in the coma are not well-known quantities. Figure 1 shows an exemple of the electron density and temperature profiles used by *Biver et al.* (1999a) for modeling excitation by collisions with electrons. These profiles are based on measurements made *in situ* in Comet Halley, and the dependences with H_2O production rate and heliocentric distance expected from theoretical modeling.

3.1.6. Non-steady-state calculations. The evolution of the population distribution with distance to the nucleus has been studied for a number of molecules: CO (*Chin and Weaver,* 1984; *Crovisier and Le Bourlot,* 1983), H_2O (*Bockelée-Morvan,* 1987), HCN (*Bockelée-Morvan et al.,* 1984), H_2CO (*Bockelée-Morvan and Crovisier,* 1992), CH_3OH (*Bockelée-Morvan et al.,* 1994), and linear molecules (*Crovisier,* 1987). Collisional excitation by electrons was included in more recent works (e.g., *Biver et al.,* 1999a). These studies solve the time-dependent equations of statistical equilibrium, as the molecules expand in the coma

$$\frac{dn_i}{dt} = -n_i \sum_{j \neq i} p_{ij} + \sum_{j \neq i} n_j p_{ji} \quad (6)$$

where the transition rate p_{ij} from level i to j, of energy E_i and E_j respectively, may involve collisional excitation (C_{ij}), radiative excitation (g_{ij}), and/or spontaneous decay (A_{ij}) terms. If we omit radiation trapping effects

$$p_{ij} = C_{ij} + g_{ij} \quad \text{if } E_i < E_j \quad (7)$$

$$p_{ij} = C_{ij} + A_{ij} \quad \text{if } E_i > E_j \quad (8)$$

The coupled differential equations (equation (6)) are "stiff", as they contain rates with time constants differing by several orders of magnitude, and their solution requires special techniques, such as the Gear method (cf. *Chin and Weaver,* 1984). In contrast, the fluorescence equilibrium solution can be simply computed by matrix inversion.

Figure 1 shows the evolution of the population of the lowest rotational levels of the HCN molecule with distance to the nucleus. At some distance in the coma, collision excitation can no longer compete with rotational spontaneous decay, and the population distribution evolves to fluorescence equilibrium. Because radiative lifetimes vary among the levels, the departure from local thermal equilibrium (LTE) occurs separately for each rotational level. The size of the LTE region also varies greatly among molecules, as shown in *Crovisier* (1987), where the evolution of the rota-

tional population distribution is computed for a number of linear molecules. Molecules with small dipole moments (e.g., CO) have long rotational lifetimes and correspondingly larger LTE regions. Symmetric molecules with no dipole moment, such as CO_2, cannot relax to low rotational levels; high rotational levels become more and more populated as the molecules expand in the coma.

Low-lying rotational levels maintain thermal populations up to a few 10^3 km from the nucleus in moderately active comets ($Q_{H_2O} \approx 10^{29}$ molecules s^{-1}) near 1 AU from the Sun. This implies that the thermal approximation is a good one to describe the rotational structure of vibrational bands observed by long-slit spectroscopy (section 3.3). On the other hand, the thermal equilibrium approximation may not be valid for the interpretation of rotational line emission observed in the radio range, owing to the large beam size of radio antennas.

3.2. Rotational Line Intensities

When rotational lines are optically thin and spontaneous emission dominates over absorption of the continuum background and stimulated emission, their line flux F_{ul} (in W m^{-2} or Jy km s^{-1}) is given by

$$F_{ul} = \frac{\Omega}{4\pi} h\nu_{ul} A_{ul} \langle N_u \rangle \qquad (9)$$

where Ω is the solid angle subtended by the main beam of the antenna. (The diffraction-limited beam pattern of circular radio antennae is well approximated by a two-dimensional gaussian, which width at half power defines the main-beam solid angle.) $\langle N_u \rangle$ is the column density within the upper transition state u, and is obtained by volume integration over the beam pattern of the density times the fractional population in the upper state. When n_u is constant within the beam, $\langle N_u \rangle$ is equal to $n_u \langle N \rangle$, where $\langle N \rangle$ is the total molecular column density that is related to the molecular production rate (section 4).

In the radio domain, line intensities are usually expressed in term of *equivalent brightness temperatures* T_B, where T_B is related to F_{ul} through the Rayleigh-Jeans limit ($h\nu \ll kT$) of the Planck function. The line area integrated over velocity in K km s^{-1} is then related to the column density through

$$\int T_B dv = \frac{hc^3 A_{ul}}{8\pi k \nu_{ul}^2} \langle N_u \rangle \qquad (10)$$

In most observational cases, radio antennas are sensitive to molecules present in the intermediate region between thermal and fluorescence equilibrium. Time-dependent excitation models, as described in section 3.1.6, are thus required to derive $\langle N \rangle$ from the observed line area $\int T_B dv$. Because these models rely on ill-known collisional excitation parameters (section 3.1.5), observers try, as much as possible, to observe several rotational lines of the same molecule. This permits them to determine the rotational temperature that best describes the relative population of the upper states, given the observed line intensities. The inferred rotational temperature can then be compared to that predicted from modeling, thereby constraining the free parameters of the model. Methanol has multiplets at 165 and 157 GHz that sample several rotational levels of same quantum number J. Their observations are particularly useful, as the rotational temperature derived from these lines is similar to the kinetic temperature in the collisional region (*Bockelée-Morvan et al.,* 1994; *Biver et al.,* 1999a, 2000). This is also the case of the 252-GHz lines shown in Fig. 2. Other series of lines (e.g., the 145- or 242-GHz multiplets of CH_3OH, or the HCN lines) exhibit rotational temperatures that are intermediate between the kinetic temperature of the inner coma and the rotational temperature at fluorescence equilibrium. These lines can be used to constrain the collision rates. Constraints can also be ob-

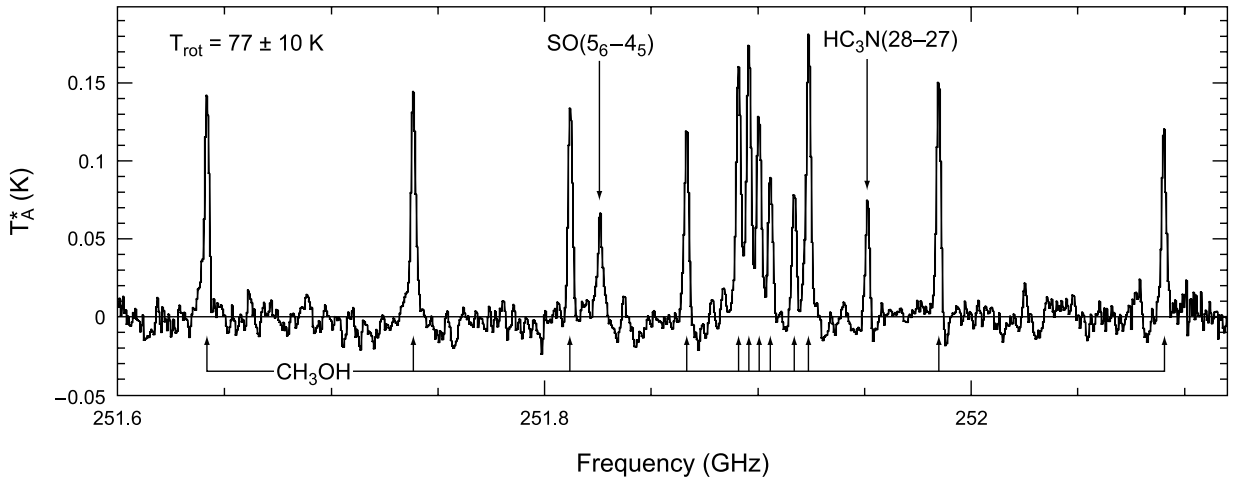

Fig. 2. Wideband spectrum of Comet Hale-Bopp observed on February 21.7, 1997 at the CSO showing twelve J_3–J_2 A lines of CH_3OH, the 5_6–4_5 line of SO, and, in the image sideband at 254.7 GHz, the J(28–27) line of HC_3N (*Lis et al.,* 1999).

tained from observations at offset positions from the nucleus (*Biver et al.,* 1999a).

Most rotational lines observed in comets are optically thin because of small molecular column densities. The only exceptions encountered were the J(4–3) HCN line observed in C/1996 B2 (Hyakutake) (*Lis et al.,* 1997; *Biver et al.,* 1999a) and Hale-Bopp (*Meier et al.,* 1998b), the H_2O rotational lines observed with ISO in Comet Hale-Bopp (*Crovisier et al.,* 1997), and the 1_{10}–1_{01} line of H_2O observed with the SWAS and Odin satellites in a few comets (*Neufeld et al.,* 2000; *Lecacheux et al.,* 2003). For the H_2O 1_{10}–1_{01} line, self-absorption effects result in asymmetric line shapes, indeed observed in high-resolution spectra obtained with Odin (*Lecacheux et al.,* 2003).

3.3. Intensity of Ro-Vibrational Lines and Vibrational Bands

As for pure rotational lines, the line flux F_{ul} (W m^{-2}) of optically thin ro-vibrational lines u → l (u within v', l within v") is given by equation (9), where Ω is the solid angle corresponding to the field of view. F_{ul} can be also expressed as a function of the emission rate (the so-called g-factor) of the line $g_{ul} = A_{ul} n_u$ (s^{-1}), assuming n_u to be constant within the field of view

$$F_{ul} = \frac{\Omega}{4\pi} h\nu_{ul} g_{ul} \langle N \rangle \qquad (11)$$

Neglecting collisional excitation, the emission rate g_{ul} is related to the fractional populations n_j within the ground vibrational state v = 0 through

$$g_{ul} = A_{ul} \frac{\sum_{j,v=0} n_j g_{ju}}{\sum_{v} \sum_{j} A_{uj}} \qquad (12)$$

where the summation in the denominator is made over all possible vibrational decays (v' → v = 0 and v' → v hot-bands, including the v' → v = v" band to which the u → l transition belongs). In the righthand term of equation (12), the g_{ju} coefficients are the excitation rates due to solar pumping defined in equation (2). Equation (12) is readily obtained by solving equation (6) for the n_u population within v', assuming steady-state (section 3.1.1) and neglecting rotational decay within v', which is much slower than vibrational decays.

The band flux is related to the total emission rate of the band $g_{v'v"}$ through a formula similar to equation (11). In the case of pure resonance fluorescence, $g_{v'v"}$ is equal to the band excitation rate $g_{v"v'}$ given in equation (3).

In most cases, individual g-factors are computed assuming LTE in the ground vibrational state. The retrieved molecular column densities (and production rates) may then depend strongly on the assumed rotational temperature. In Comet Hale-Bopp and other bright comets, many ro-vibrational lines were observed for most molecules, allowing measurement of the rotational temperature T_{rot} and an accurate derivation of the production rate. Figure 3 shows the H_2O ν_3 band of H_2O observed with ISO in Comet Hale-Bopp at 2.9 AU from the Sun (*Crovisier et al.,* 1997), and the synthetic spectrum that best fits the data with T_{rot} = 29 K. Figure 4 shows examples of groundbased IR spectra for Comets Hyakutake and C/1999 H1 (Lee) at r ~ 1 AU, where several lines of H_2O and CO are detected: From Boltzmann analyses of the line intensities, T_{rot} was estimated to ~75 K for both comets (*Mumma et al.,* 2001b).

Opacity effects in the solar pump and for the emitted photons, if present, would affect the effective line-by-line infrared fluorescence emission rates and the intensity distribution within the bands. This was investigated by *Bockelée-Morvan* (1987) for the ν_2 and ν_3 bands of H_2O, and accounted for in the determination of the ortho-to-para ratio of H_2O from the ISO spectra (*Crovisier et al.,* 1997) (Fig. 3; section 10). The opacity of the CO_2 ν_3 band observed by VEGA/IKS in 1P/Halley was taken into account for accurate measurement of the CO_2 production rate in this comet (*Combes et al.,* 1988). Since optical depth effects are stronger in the inner coma, the spatial brightness profile of an optically thick line falls off less steeply with distance to the nucleus than under optically thin conditions. Optical depths of OCS ν_3 and CO v(1–0) ro-vibrational lines were evaluated (*Dello Russo et al.,* 1998; *DiSanti et al.,* 2001; *Brooke et al.,* 2003), in order to investigate whether this could explain their relatively flat spatial brightness distributions in Comet Hale-Bopp (section 7), but the effect was found to be insignificant.

3.4. Electronic Bands

The parent molecules studied via electronic bands at UV/FUV wavelengths are CO, S_2, and, indirectly, CO_2 (Fig. 5). Two other potential constituents of the nucleus, H_2 and N_2, can also fluoresce at UV and FUV wavelengths. H_2 was recently detected during observations of two long-period comets with the Far Ultraviolet Spectroscopic Explorer (FUSE); however, the amount measured was consistent with all the H_2 being derived from the photolysis of H_2O, rather than from sublimation of frozen H_2 in the nucleus (*Feldman et al.,* 2002). Further discussion of cometary H_2 can be found in *Feldman et al.* (2004). Although electronic excitation of N_2 usually leads to predissociation, fluorescence can occur in the (0,0) band of the Carroll-Yoshino system ($c4'^1\Sigma_u^+$–$X^1\Sigma_g^+$) at 958.6 Å. Several cometary spectra were taken with FUSE to search for fluorescence from N_2, but only upper limits were derived (P. D. Feldman, personal communication, 2003) (see section 5.6.1).

Observations of CO in the UV range are discussed in section 5.2. The calculation of g-factors for the CO A–X bands is discussed by *Tozzi et al.* (1998), and g-factors for the B–X, C–X, and E–X bands are discussed by *Feldman et al.* (2002). Generally, the Swings effect (see section 3.1.2) is small for all the UV bands of CO, with g-factor variations of only ~20% with heliocentric radial velocity.

Emission in the CO Cameron band system near 2050 Å ($a^3\Pi$–$X^1\Sigma^+$) was discovered during Hubble Space Telescope

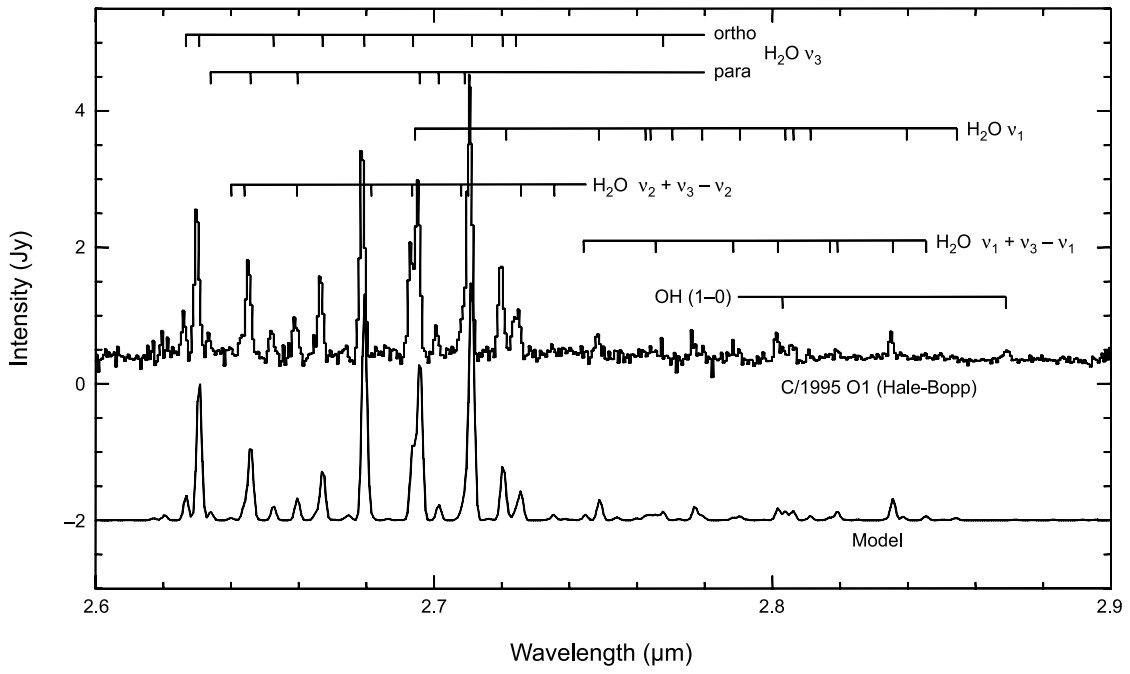

Fig. 3. The region of the ν_3 band of water observed with the ISO short-wavelength spectrometer in Comet C/1995 O1 (Hale-Bopp) on 27 September and 6 October 1996 (top). Line assignations are indicated. The synthetic fluorescence spectrum of water that is the best fit to the data (bottom) corresponds to $Q(H_2O) = 3.6 \times 10^{29}$ molecules s^{-1}, $T_{rot} = 28.5$ K and OPR = 2.45. Adapted from *Crovisier et al.* (1997).

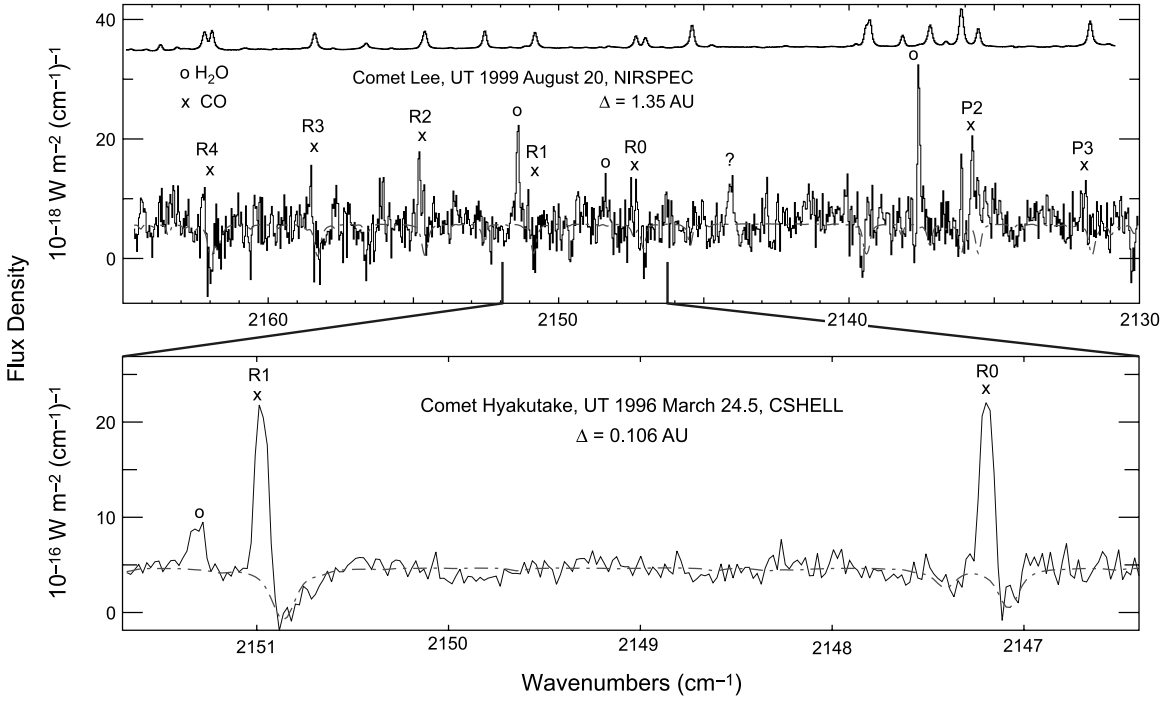

Fig. 4. Detection of CO and H_2O in Comets C/1996 B2 (Hyakutake) and C/1999 H1 (Lee) in the 4.7-μm region (from *Mumma et al.,* 2001b). Several lines of the CO ν(1–0) and H_2O ν_1–ν_2 and ν_3–ν_2 bands are present. The relative intensities of CO and H_2O lines are reversed even though the rotational temperatures were similar for the two comets, providing graphic evidence of the dramatically different CO abundance in these two comets.

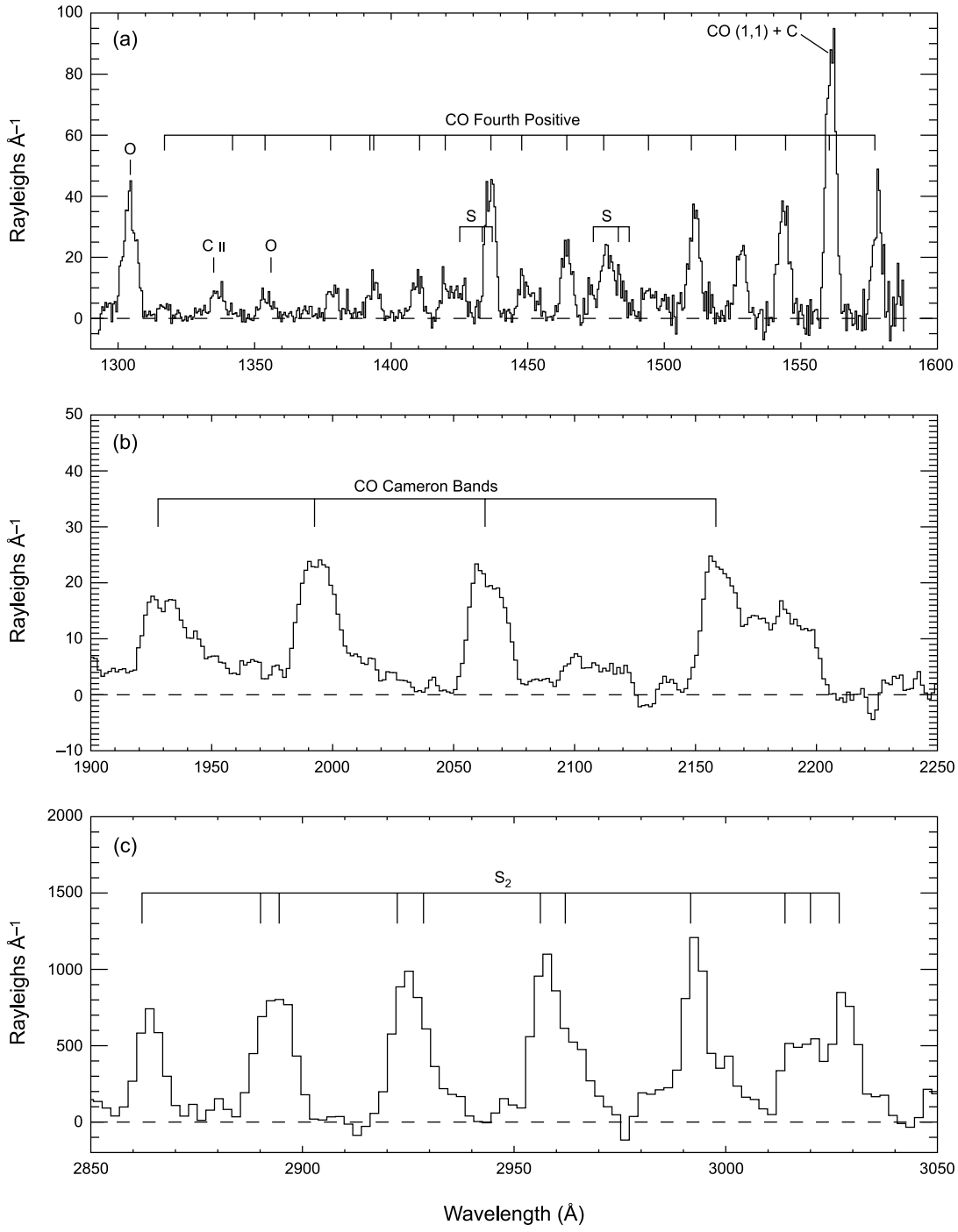

Fig. 5. Portions of the ultraviolet (UV) spectra of C/1996 B2 (Hyakutake) taken on 1996 April 1 with the HST. All the parent molecules detected at UV wavelengths are represented: The top panel shows multiple bands in the Fourth Positive Group of CO; the middle panel shows several bands of the CO Cameron system, which is thought to be produced mainly by prompt emission following the photodissociation of CO_2, and the bottom panel shows multiple bands of the B–X system of S_2. Figure adapted from *Weaver* (1998).

(HST) observations of 103P/Hartley 2 (*Weaver et al.,* 1994), and this spurred a reanalysis of earlier data acquired with the International Ultraviolet Explorer (IUE) that resulted in the detection of Cameron band emission in several other comets (*Feldman et al.,* 1997). The Cameron bands involve transitions between triplet and singlet electronic states, i.e., they are electric dipole forbidden, which means that resonance fluorescence cannot be the excitation mechanism. The Cameron bands can be excited during the photodissociation of CO_2, producing CO molecules in the $a^3\Pi$ state that can then decay to the ground state on a timescale of ~10 ms in a process called *prompt* emission (*Weaver et al.,*

1994). In this case, the CO Cameron band emission is directly proportional to the CO_2 production rate, and its intensity can be used to estimate the CO_2 abundance in exactly the same way that observations of the O^1D line near 6300 Å can be used to probe the H_2O production rate (cf. *Feldman et al.,* 2004). Unfortunately, electron impact on CO also produces Cameron band emission fairly efficiently, and this complicates the interpretation of the spectra when both CO and CO_2 are comparably abundant. When spectra are taken at sufficient resolution to resolve the rotational structure in the Cameron bands, the two competing excitation mechanisms can be easily distinguished because the CO molecules produced during the photolysis of CO_2 are rotationally "hot", with a rotational temperature about five times larger than for the CO excited by electron impact (*Mumma et al.,* 1975).

S_2 has been observed through its $B^3\Sigma_u^- – X^3\Sigma_g^-$ system in the near-UV in several comets (section 5.5). Because of its very short lifetime (≈500 s), S_2 is concentrated within a small spatial region near the nucleus and observations with high spatial resolution (≲500 km) are required to detect it. The photodissociation rate and the B–X g-factor of S_2 are comparable. Thus, a time-dependent model of the excitation is required for accurate interpretation of the emission (*Kim et al.,* 2003; *Reylé and Boice,* 2003).

Cometary emission in electronic bands is generally produced by resonance fluorescence, as are the great majority of cometary emissions observed at optical and near-IR wavelengths. However, the anomalous intensity ratio of the CO C–X and B–X bands in the FUSE spectrum of C/2001 A2 (LINEAR) suggests that some of the B–X emission is produced by e^--impact on CO, while the presence of a "hot" component in the C–X emission is suggestive of an excitation process involving CO_2 (*Feldman et al.,* 2002). As previously discussed, the CO Cameron bands can be excited by both photodissociative and e^--impact processes.

4. DETERMINATION OF PRODUCTION RATES

For estimating relative molecular abundances in the nucleus, the measured column densities (or local densities in the case of *in situ* measurements) are converted into molecular production rates, i.e., outgassing rates at the nucleus. This step requires a good description of the molecular spatial distributions. Most studies use the Haser model (*Haser,* 1957), which assumes that the parent molecule is sublimating from the surface of the nucleus at a constant rate and expands radially outward at constant velocity. Under these conditions, the local density in the coma n is given by

$$n(r_c) = \frac{Q}{4\pi r_c^2 v} e^{-(r_c - r_n)/v\tau} \qquad (13)$$

where Q is the production rate, r_c is the distance from the center of the nucleus, r_n is the radius of the nucleus, v is the outflow speed, and τ is the molecular lifetime. The density is then integrated along the line of sight to obtain the column density.

For the case of a circular observing aperture centered on the nucleus, if the aperture subtends a distance at the comet that is much smaller than the scalelength (L = vτ) of the molecule, the average column density within the aperture is given by

$$\langle N \rangle = \frac{Q}{vd} \qquad (14)$$

where d is the aperture diameter.

If the aperture size is much larger than the scalelength of the molecule, then

$$\langle N \rangle = \frac{4Q\tau}{\pi d^2} \qquad (15)$$

When equations (14) and (15) are not applicable, other methods must be used to relate the column density to the production rate. While convenient tabulations are available for both circular (*Yamamoto,* 1982) and square (*Hoban et al.,* 1991) apertures, the continually increasing power of computers makes the direct integration of equation (13) simple, fast, and accessible to most researchers.

In the limit cases of equations (14) and (15), ⟨N⟩ depends on either v or τ. In the intermediate cases, the column density depends on both the lifetime and velocity. Lifetimes have been computed for many parent molecules (*Huebner et al.,* 1992; *Crovisier,* 1994) under both solar maximum and solar minimum conditions and have accuracies of ~20–30% for the well-documented species. But the photodissociation rates of several cometary molecules (e.g., H_2CS, SO_2, NH_2CHO) are unavailable or uncertain by factors of several. Expansion velocities for some molecules can be determined from analysis of observed radio line profiles, but usually the outflow velocities are uncertain by ~30%. There is also the problem that the outflow velocity changes with position in the coma, as molecules are accelerated by photolytic heating in the coma, but typically observers adopt an average outflow speed that is appropriate for the size of the aperture used (i.e., smaller velocities used for smaller apertures).

For molecules released by an extended source, such as H_2CO (section 7), the Haser formula for daughter species (see *Combi et al.,* 2004) is generally used to describe their spatial distribution. Inferred production rates then strongly depend on the scalelength of their parent source, L_p, especially when the field of view samples cometocentric distances smaller than L_p. Any underestimate of L_p will result in an underestimate of the production rate. In this context, there are some uncertainties in the production rates derived from radio observations of distant comets for which sublimation from icy grains is likely and not taken into account in most studies (*A'Hearn et al.,* 1984; *Biver et al.,* 1997; *Womack et al.,* 1997; *Gunnarsson et al.,* 2002). H_2CO production rates obtained in Comet Hale-Bopp at large r are uncertain as well, as there is little information on the he-

liocentric variation of the H_2CO parent scalelength (see section 7).

With sufficient spatial resolution and mapping, the radial distribution of molecules can be investigated, and production rates can be more accurately determined. Section 7 discusses how native and extended sources of CO molecules are extracted from the analysis of long-slit spectra.

The spatial distribution of cometary molecules is certainly much more complex than assumed by the Haser model. As discussed elsewhere in this book (e.g., *Crifo et al.,* 2004), the production rate may vary on short timescales, outgassing from the nucleus may not be isotropic, and the expansion velocity increases with distance from the nucleus and may have day/night asymmetries. Anisotropic outgassing and/or velocity variations have been considered in a few radio studies, using information provided by the line shapes and mapping (e.g., *Gunnarsson et al.,* 2002; *Veal et al.,* 2000).

5. OBSERVATIONS OF PARENT MOLECULES

In this section, we review the *in situ* measurements and spectroscopic investigations of parent molecules and noble gases. The production rates relative to H_2O (also called abundances in the text) measured in several well-documented comets near their perihelion are listed in Table 1. Upper limits for several undetected molecules are given in Table 2.

5.1. Water

Water is the most abundant constituent of cometary ices and its production rate is used for quantifying cometary activity and for abundance determinations. Its presence in cometary comae was definitively established in the 1970s from observations of H and OH, which showed that these species were produced in appropriate quantities and with spatial distributions and velocities consistent with H_2O photolysis (see the review of *Festou et al.,* 1993).

Water is difficult to measure directly. The fundamental bands of vibration, especially ν_3 near 2.7 μm, cannot be observed from the ground because of strong absorption in the terrestrial atmosphere. This band was observed in 1P/Halley and C/1986 P1 (Wilson) from the KAO (*Mumma et al.,* 1986; *Larson et al., 1*989), in 1P/Halley with the *Vega*/IKS IR spectrometer (*Combes et al.,* 1988), and with ISO in Comets Hale-Bopp and 103P/Hartley 2 (*Crovisier et al.,* 1997, 1999a,b) (Fig. 3).

Nonresonance fluorescence bands (hot-bands) of H_2O have weaker g-factors, but some are not absorbed by telluric H_2O and thus can be observed from the ground. Direct absorption of sunlight excites molecules from the ground vibrational state to a higher vibrational state, followed by cascade into an intermediate level that is not significantly populated in the terrestrial atmosphere (*Crovisier,* 1984). Hot-band emission from H_2O $\nu_2 + \nu_3 - \nu_2$ was first detected near 2.66 μm in high-dispersion airborne IR spectra of Comets 1P/Halley and C/1986 P1 (Wilson) (*Weaver et al.,* 1986; *Larson et al.,* 1989), but the strong 2.7-μm fundamental bands (ν_1 and ν_3) blanket this entire region from the ground. However, groundbased IR observations of Comets 1P/Halley and C/1986 P1 (Wilson) indicated the presence of excess flux near 2.8 μm that could not be attributed to H_2O fundamental bands (*Tokunaga et al.,* 1987; *Brooke et al.,* 1989), but was consistent with the expected flux from H_2O hot-bands (*Bockelée-Morvan and Crovisier,* 1989). The hot-band emissions in this spectral region were more extensively sampled by ISO in Comet Hale-Bopp (Fig. 3). High spectral dispersion surveys of the 2.9-μm region obtained in Comets C/1999 H1 (Lee) and 153P/2002 C1 (Ikeya-Zhang) with NIRSPEC at the Keck telescope revealed multiple lines of the $\nu_1 + \nu_3 - \nu_1$, $(\nu_1 + \nu_2 + \nu_3) - (\nu_1 + \nu_2)$, and $2\nu_1 - \nu_1$ H_2O hot-bands (*Mumma et al.,* 2001a; *Dello Russo et al.,* 2004).

In other spectral regions, the terrestrial atmosphere is generally transparent to H_2O hot-band emissions. Hot-band emission from H_2O was detected in Comets C/1991 T2 (Shoemaker-Levy), 6P/d'Arrest, and C/1996 B2 (Hyakutake) using bands near 2 μm ($\nu_1 + \nu_2 + \nu_3 - \nu_1$ and $2\nu_2 + \nu_3 - \nu_2$) (*Mumma et al.,* 1995, 1996; *Dello Russo et al.,* 2002a). Production rates were obtained for all three comets, and a rotational temperature was obtained for H_2O in Comet Hyakutake (*Mumma et al.,* 1996). A survey of the CO (1–0) band (4.7 μm) in Comet Hyakutake revealed new emissions that were identified as nonresonance fluorescence from the $\nu_1 - \nu_2$ and $\nu_3 - \nu_2$ hot-bands of H_2O (*Mumma et al.,* 1996; *Dello Russo et al.,* 2002a). As H_2O and CO can be sampled simultaneously (Fig. 4), preference was given to the 4.7-μm region thereafter (e.g., C/1995 O1 Hale-Bopp (*Weaver et al.,* 1999b; *Dello Russo et al.,* 2000), 21P/Giacobini-Zinner (*Weaver et al.,* 1999a; *Mumma et al.,* 2000), C/1999 H1 (Lee) (*Mumma et al.,* 2001b), C/1999 S4 (LINEAR) (*Mumma et al.,* 2001a).

The rotational lines of H_2O also cannot be observed from the ground, except for a line of one of the trace isotopes (HDO — see section 9). Lines in the far-IR, especially the 2_{12}–1_{01}, 2_{21}–2_{12} and 3_{03}–2_{12} lines near 180 μm, were observed by ISO in Comet Hale-Bopp (*Crovisier et al.,* 1997). The fundamental ortho rotational line, 1_{10}–1_{01} at 557 GHz, was observed using SWAS (*Neufeld et al.,* 2000) and the Odin satellite (*Lecacheux et al.,* 2003) in C/1999 H1 (Lee), 153P/2002 C1 (Ikeya-Zhang), and several other comets. These lines are very optically thick, which means that the derivation of accurate H_2O production rates requires a reliable model for the H_2O excitation and radiative transfer.

5.2. Carbon Monoxide and Carbon Dioxide

5.2.1. Carbon monoxide (CO). The CO molecule was discovered in comets during a sounding rocket observation of C/1975 V1 (West), when resonance fluorescence in the Fourth Positive Group ($A^1\Pi$–$X^1\Sigma^+$) near 1500 Å was detected in the UV spectrum (*Feldman and Brune,* 1976). Emission in these bands has been detected subsequently in nearly every bright ($m_V < 7$) comet observed at UV wavelengths with IUE (cf. *Feldman et al.,* 1997), the HST (cf.

TABLE 1. Production rates relative to water in comets.

Molecule	1P/Halley	C/1995 O1 (Hale-Bopp)	C/1996 B2 (Hyakutake)	C/1999 H1 (Lee)	C/1999 S4 (LINEAR)	153P/2002 C1 (Ikeya-Zhang)
H_2O	100	100	100	100	100	100
CO	3.5*, 11[1]	12*,[13], 23[13,14]	14*,[25,26], 19–30[25,27,28]	1.8[36]–4[37]	≤0.4[41], 0.9[42]	2[45], 4–5[46,47]
CO_2	3–4[2,3]	6†,15				
CH_4	<0.8[4]	1.5[16]	0.8[16,29]	0.8[38]	0.14[42]	0.5[16]
C_2H_2	0.3[1]	0.1[16]–0.3[17]	0.2[30]–0.5[31]	0.27[38]	<0.12[42]	0.18[48]
C_2H_6	0.4[1]	0.6[17]	0.6[29]	0.67[38]	0.11[42]	0.62[49]
CH_3OH	1.8[5,6]	2.4[14]	2[27,28]	2.1[38]–4[39]	<0.15[42]	2.5[46,47]
H_2CO‡	4[2,7,8]	1.1[14]	1[27,28]	1.3[39]	0.6[41]	0.4[47]
HCOOH		0.09[14]				<0.1[43]
$HCOOCH_3$		0.08[14]				
CH_3CHO		0.02[18]				
NH_2CHO		0.015[14]				
NH_3	1.5[9]	0.7[19]	0.5[32,33]			<0.2[50]
HCN	0.1[10,11]	0.25[14,20]	0.1[27,28]–0.2[34]	0.1[38]–0.3[39]	0.1[42]	0.1[47]–0.2[48]
HNCO		0.10[14]	0.07[28]			0.04[47]
HNC		0.04[14,21]	0.01[28,35]	0.01[39]	0.02[43]	0.005§,[47]
CH_3CN		0.02[14]	0.01[33]			0.01[47]
HC_3N		0.02[14]				<0.01[47]
H_2S	0.4[6]	1.5[14]	0.8[27]	<0.9[39]	0.3[43]	0.8[47]
OCS		0.4[14,22]	0.1[36]			<0.2[47]
SO_2		0.2[14]				
CS_2	0.2[12]	0.2[14]	0.1[27]	0.08[39]	0.12[43]	0.06[47]–0.1[45]
H_2CS		0.05[23]				
NS		≥0.02[24]				
S_2			0.005[37]	0.002[40]	0.0012[44]	0.004[45]

*Production from the nucleus; see text.

†Value at heliocentric distance r = 1 AU extrapolated from the value of 20% measured at r = 2.9 AU, assuming that $[CO_2]/[CO]$ did not change with r.

‡H_2CO abundances refer to production from an extended source.

§Measured at r ~ 1 AU; increased up to 0.02% at r ~ 0.5 AU (N. Biver et al., personal communication, 2003; *Irvine et al.,* 2003).

References: [1] *Eberhardt* (1999); [2] *Combes et al.* (1988); [3] *Krankowsky et al.* (1986); [4] *Altwegg et al.* (1994); [5] *Bockelée-Morvan et al.* (1995); [6] *Eberhardt et al.* (1994); [7] *Meier et al.* (1993); [8] *Mumma and Reuter* (1989); [9] *Meier et al.* (1994); [10] *Despois et al.* (1986); [11] *Schloerb et al.* (1986); [12] *Feldman et al.* (1987); [13] *DiSanti et al.* (2001); [14] *Bockelée-Morvan et al.* (2000); [15] *Crovisier et al.* (1997); [16] *Gibb et al.* (2003); [17] *Dello Russo et al.* (2001); [18] *Crovisier et al.* (2004a); [19] *Bird et al.* (1999); [20] *Magee-Sauer et al.* (1999); [21] *Irvine et al.* (1998); [22] *Dello Russo et al.* (1998); [23] *Woodney* (2000); [24] *Irvine et al.* (2000b); [25] *DiSanti et al.* (2003); [26] *McPhate et al.* (1996); [27] *Biver et al.* (1999a); [28] *Lis et al.* (1997); [29] *Mumma et al.* (1996); [30] *Mumma et al.* (2003); [31] *Brooke et al.* (1996); [32] *Palmer et al.* (1996); [33] *Bockelée-Morvan* (1997); [34] *Magee-Sauer et al.* (2002a); [35] *Irvine et al.* (1996); [36] *Woodney et al.* (1997); [37] *Weaver et al.* (1996); [38] *Mumma et al.* (2001b); [39] *Biver et al.* (2000); [40] *Feldman et al.* (1999); [41] *Weaver et al.* (2001); [42] *Mumma et al.* (2001a); [43] *Bockelée-Morvan et al.* (2001); [44] *Weaver* (2000); [45] *Weaver et al.* (2002b); [46] *DiSanti et al.* (2002); [47] N. Biver et al. (personal communication, 2003); [48] *Magee-Sauer et al.* (2002b); [49] *Dello Russo et al.* (2002b); [50] *Bird et al.* (2002).

Weaver, 1998), and sounding rockets (cf. *Feldman,* 1999). More recently, resonance fluorescence in several bands of the Hopfield-Birge system ($B^1\Sigma^+$–$X^1\Sigma^+$, $C^1\Sigma^+$–$X^1\Sigma^+$, and $E^1\Pi$–$X^1\Sigma^+$) has been detected between 1075 Å and 1155 Å in spectra measured by FUSE (*Feldman et al.,* 2002). Through the end of 2002, CO emission had been detected in a total of 12 comets at UV wavelengths, with $[CO/H_2O]$ abundances ranging from ~0.4% to nearly 30%.

The radio lines of CO are intrinsically weak because of the small dipole moment of this molecule. However, these lines are the most easily detected gaseous emissions for comets at large heliocentric distances (r ≥ 3 AU). The CO J(2–1) line at 230 GHz was first observed in 29P/Schwassmann-Wachmann 1 (*Senay and Jewitt,* 1994) at r ≈ 6 AU, and subsequently in a few bright comets. In Comets Hyakutake and Hale-Bopp, the J(1–0) and J(3–2) lines were also observed. The J(2–1) line was detected out to r = 14 AU in Comet Hale-Bopp with the Swedish-ESO Submillimetre Telescope (SEST) (*Biver et al.,* 2002a).

The first clear detection of the lines of the v(1–0) IR band of CO near 4.7 μm was obtained during observations of Comet Hyakutake (*Mumma et al.,* 1996; *DiSanti et al.,* 2003). Eight lines of this band were detected in emission, using CSHELL spectrometer at the NASA/IRTF. CO has

TABLE 2. Molecular upper limits in Comet Hale-Bopp from radio observations (from *Crovisier et al.,* 2004).

Molecule	(X)/(H_2O)
H_2O	100
H_2O_2	<0.03
CH_3CCH	<0.045
CH_2CO	<0.032
C_2H_5OH	<0.10
CH_3OCH_3	<0.45
CH_3COOH	<0.06
Glycine I	<0.15
HC_5N	<0.003
C_2H_5CN	<0.01
CH_2NH	<0.032
CH_3SH	<0.05
NaOH	<0.0003
NaCl	<0.0008

been detected in every comet observed since then with CSHELL and with NIRSPEC at the Keck Observatory (eight Oort cloud comets and one Jupiter-family comet) (*Mumma et al.,* 2003; *Weaver et al.,* 1999a,b). Selected spectra of C/1999 H1 (Lee) and Comet Hyakutake are shown in Fig. 4. CO rotational temperatures were obtained from Boltzmann analyses of the measured spectral line intensities and were used to extrapolate total production rates from the observed lines. For eight Oort cloud comets observed by IR ground-based spectroscopy through the end of 2002, the total CO abundance ranged from 1% to 24% relative to H_2O (*Mumma et al.,* 2003).

CO was investigated by mass spectrometry in 1P/Halley with the *Giotto* NMS (*Eberhardt et al.,* 1987). As detailed in section 7.1, these measurements revealed that part of the CO originated from an extended source. Native and extended sources of CO were separately quantified in a few comets from long-slit IR observations (section 7.2). Among eight Oort cloud comets observed at IR wavelengths, the native abundance [CO/H_2O] varies by more than a factor of 40 [0.4–17% (*Mumma et al.,* 2003) (section 8).

5.2.2. Carbon dioxide (CO_2). The presence of carbon dioxide in cometary comae was indirectly established a long time ago from the existence of CO_2^+ in cometary tails (see *Feldman et al.,* 2004). It was confirmed by the detection of the CO_2 ν_3 band at 4.26 μm. This band is very strong (g-factor = 2.6×10^{-3} s^{-1}), but it cannot be observed from the ground because of strong absorption from terrestrial CO_2. The ν_3 band has only been observed by *Vega*/IKS in 1P/Halley (*Combes et al.,* 1988), and by ISO in Comets Hale-Bopp (*Crovisier et al.,* 1997, 1999a) and 103P/Hartley 2 (*Colangeli et al.,* 1999; *Crovisier et al.,* 1999b). CO_2 was also observed in 1P/Halley from the mass 44 peak in the *Giotto* NMS mass spectra (*Krankowsky et al.,* 1986). The inferred CO_2 production rate relative to H_2O was 3–4% in 1P/Halley and 8–10% in 103P/Hartley 2. It was >20% in Comet Hale-Bopp, but this comet was only observed at r > 2.9 AU. This higher value is likely due to the higher volatility of CO_2 compared to H_2O. The value of 6% given in Table 1 is that extrapolated to 1 AU, using the $Q(CO_2)/Q(CO)$ ratio of ~0.3 measured at 2.9 AU.

As discussed in section 3.4, the presence of CO_2 is also indirectly inferred from observations of the CO Cameron bands near 2050 Å, which can be emitted via prompt emission following the photodissociation of CO_2. In practice, these UV bands can only be used to derive accurate CO_2 production rates when the comet is CO-depleted, or is bright enough to allow observations with sufficient spectral resolution ($\lambda/\delta\lambda \geq 1500$) to unambiguously identify the separate emissions from CO_2 photodissociation and electron impact on CO, which overlap in low-resolution data.

5.3. Methanol (CH_3OH), Formaldehyde (H_2CO), and Other CHO-bearing Molecules

5.3.1. Methanol (CH_3OH). The identification of CH_3OH was first suggested by *Knacke et al.* (1986) to explain the 3.52-μm feature seen near the broad 3.3–3.5-μm emission in several low-resolution spectra of 1P/Halley. *Hoban et al.* (1991) observed the 3.52-μm feature in Comets C/1989 Q1 (Okazaki-Levy-Rudenko), C/1989 X1 (Austin), C/1990 K1 (Levy), and 23P/Brorsen-Metcalf, and showed that its properties were consistent with fluorescence from low-temperature (70 K) CH_3OH in the ν_3 band. Figure 6 displays 3.2–3.7-μm spectra of Comets C/1989 X1 (Austin) and C/1990 K1 (Levy) showing CH_3OH emission. Definite identification of CH_3OH in cometary comae was obtained from the detection of several J(3–2) rotational lines at 145 GHz in Comets C/1989 X1 (Austin) and C/1990 K1 (Levy) at the 30-m telescope of the Institut de Radioastronomie Millimétrique (IRAM) (*Bockelée-Morvan et al.,* 1991, 1994).

Methanol has now been observed in many comets, both at radio and IR wavelengths, and the CH_3OH abundances inferred from radio and IR spectra are generally consistent (Table 1). In Comet Hale-Bopp, ~70 rotational lines were detected at millimeter and submillimeter wavelengths (*Biver et al.,* 1999b). Methanol rotational lines often appear as multiplets in radio spectra (Fig. 2), whose analysis provides clues to the temperature and excitation conditions in the coma (see section 3.2). High-resolution Keck/NIRSPEC spectra obtained in the 3-μm region in Comets C/1999 H1 (Lee) and C/1999 S4 (LINEAR) show the P, Q, R structure of the ν_3 band and present, near 3.35 μm, many ro-vibrational lines belonging to the ν_2 and ν_9 CH_3OH bands (*Mumma et al.,* 2001a,b).

The ν_2 and ν_9 CH_3 stretching modes of CH_3OH are responsible for about half the total intensity of the 3.3–3.5-μm emission feature (*Hoban et al.,* 1993; *Bockelée-Morvan et al.,* 1995). Synthetic spectra, as modeled by Bockelée-Morvan et al., are shown in Fig. 6. Other weaker CH_3OH combination bands should contribute as well. The rotational structure of these bands is not yet available, which makes it difficult to identify new hydrocarbons or CHO-bearing molecules in this spectral region.

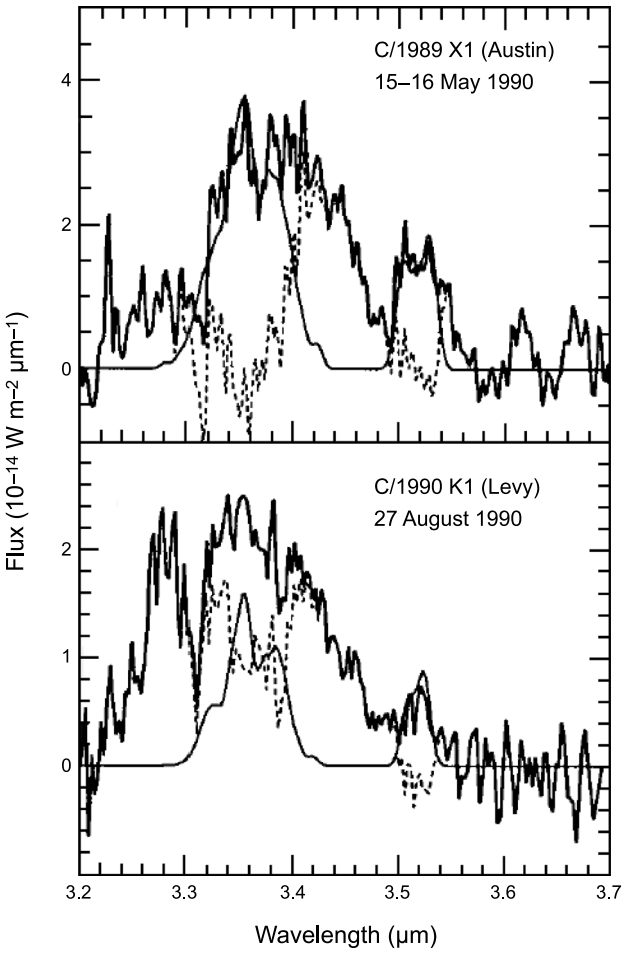

Fig. 6. 3.2–3.7-μm spectra of Comets C/1989 X1 (Austin) and C/1990 K1 (Levy) (thick line). The continuum flux due to thermal emission and scattered light from dust grains has been subtracted. The contributions of the methanol bands (ν_2, ν_3, and ν_9 at 3.33, 3.37, and 3.52 μm respectively) are shown in thin lines. The residual emission spectra, after subtracting methanol emission, are shown in dashed line. Figure adapted from *Bockelée-Morvan et al.* (1995).

Besides the 3.52-μm band, CH_3OH is identified in 1P/Halley from the peak at 33 amu/q present in *Giotto* IMS and *Giotto* NMS mass spectra, which is essentialy due to $CH_3OH_2^+$ (*Geiss et al.,* 1991; *Eberhardt et al.,* 1994). Eberhardt et al. inferred a CH_3OH abundance relative to H_2O that is consistent with the value derived from the 3.52-μm band.

The [CH_3OH/H_2O] abundance ratios measured up to now range from less than 0.15% in Comet C/1999 S4 (LINEAR) to 6%, with many comets around ~2% (see section 8).

5.3.2. Formaldehyde (H_2CO). Cometary H_2CO was first identified in 1P/Halley, from the signature of its protonated ion in mass-spectra obtained with *Giotto* NMS (*Meier et al.,* 1993). Its spatial distribution was found to differ from that expected for a parent molecule, suggesting the presence of a extended source of H_2CO in the coma (see the discussion in section 7). Its ν_1 band near 3.59 μm was possibly detected in the *Vega*/IKS spectrum of 1P/Halley (*Combes et al.,* 1988; *Mumma and Reuter,* 1989) This detection is controversial, however, as this band was not detected in groundbased IR spectra of 1P/Halley and several other comets (e.g., *Reuter et al.,* 1992). The detection of H_2CO by IR long-slit spectroscopy is difficult, owing to its low abundance and daughter-like density distribution. Recently, *DiSanti et al.* (2002) reported the detection of the Q branch of the H_2CO ν_1 band in high-resolution spectra of 153P/2002 C1 (Ikeya-Zhang) obtained with CSHELL at the NASA/IRTF.

A detection of the 1_{10}–1_{11} line of H_2CO at 6 cm wavelength in Comet 1P/Halley using the Very Large Array (VLA), announced by *Snyder et al.* (1989), is controversial. If real, it would lead to an exceptionally high abundance of H_2CO (see discussion in *Bockelée-Morvan and Crovisier,* 1992). The first definite detection of H_2CO at millimeter wavelengths (3_{12}–2_{11} at ~226 GHz) was in Comet C/1989 X1 (Austin) at IRAM (*Colom et al.,* 1992). Since then, this molecule has been observed via several lines at millimeter and submillimeter wavelengths in several comets. H_2CO was monitored at radio wavelengths in Comet Hale-Bopp (*Biver et al.,* 1997, 1999b, 2002a) (see Fig. 7). It exhibited a steep heliocentric production curve (~$r^{-4.5}$) over the entire range $1 \le r \le 4$ AU, which contrasted with the r^{-3}–r^{-2} evolution observed for most molecules. This behavior is related

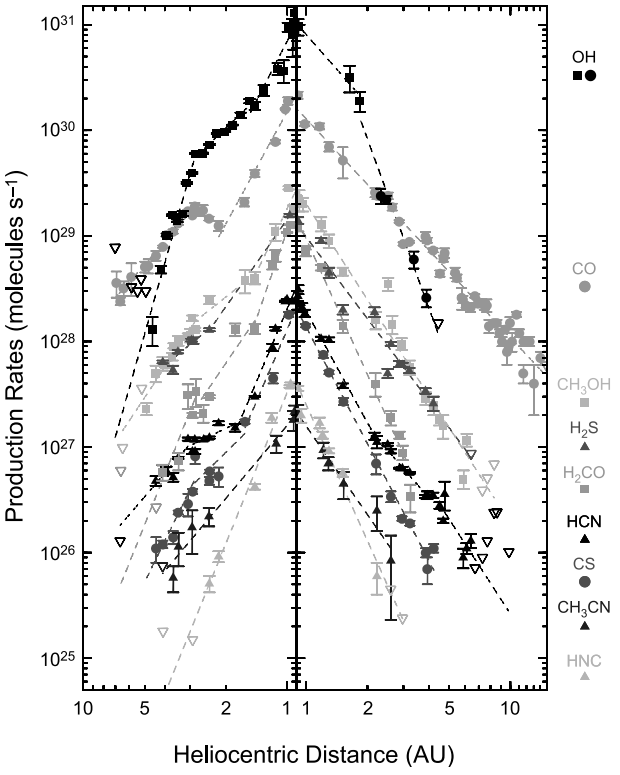

Fig. 7. Gas production curves in Comet Hale-Bopp from radio observations at IRAM, JCMT, CSO, and SEST telescopes (*Biver et al.,* 2002a). OH production rates are from observations of the 18-cm lines at the Nançay radio telescope. Inverted triangles indicate upper limits in cases of nondetection.

to the production mechanism of H_2CO, which became more efficient when the comet approached the Sun.

The $Q(H_2CO)/Q(H_2O)$ production rate ratio refering to the extended H_2CO production has been estimated to 4% for Comet 1P/Halley. This ratio ranges from 0.13 to 1.3% for comets in which H_2CO has been investigated at millimeter wavelengths (*Biver et al.,* 2002b).

5.3.3. Other CHO-bearing molecules. Several new organic CHO-bearing molecules were identified in Comet Hale-Bopp with millimeter spectroscopy thanks to its high gaseous activity. Formic acid (HCOOH) was detected from four J(10–9) lines near 225 GHz using the Plateau de Bure interferometer (PdBi) of IRAM in single dish mode (Fig. 8) (*Bockelée-Morvan et al.,* 2000). Methyl formate ($HCOOCH_3$) is one of the most complex cometary molecule detected in the gas phase. A blend of eight J(21–20) rotational transitions at ~227.56 GHz was detected in low-resolution spectra of Comet Hale-Bopp obtained at the IRAM 30-m telescope (*Bockelée-Morv*an *et al.,* 2000) (see Fig. 8). Acetaldehyde (CH_3CHO) has been detected from its $13_{0,13}$–$12_{0,12}$ A+ line at 244.83 GHz with IRAM/PdBi (*Crovisier et al.,* 2004a). Several marginal features at the frequencies of CH_3CHO lines are also present in IRAM 30-m spectra (*Crovisier et al.,* 2004a). These molecules, which are ubiquitous components of star-forming regions, are much less abundant than CH_3OH and H_2CO (Table 1): ~0.1% relative to H_2O for HCOOH and $HCOOCH_3$, and ~0.02% for CH_3CHO. Further work on archive millimeter spectra of Comet Hale-Bopp led to the identification of ethylene glycol ($HOCH_2CH_2OH$) (*Crovisier et al.,* 2004b) with an abundance of 0.25% relative to water.

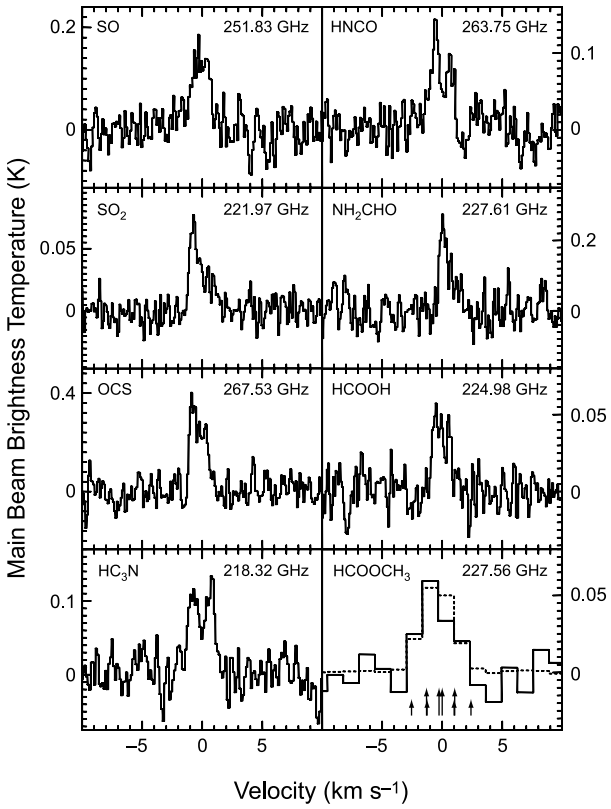

Fig. 8. Spectra of SO (CSO, February 21), SO_2 (IRAM/PdBi, March 18, 20, 21), OCS (CSO, March 26), HC_3N (CSO, February 20), HNCO (CSO, February 19), NH_2CHO (IRAM 30-m, April 5), HCOOH (IRAM/PdBi, March 20–21), and $HCOOCH_3$ (IRAM 30-m, April 5) observed in Comet Hale-Bopp in 1997. The velocity frame is with respect to the comet nucleus velocity. The dashed line superimposed on the observed spectrum of $HCOOCH_3$ is a synthetic profile, which takes into account that the $HCOOCH_3$ line at ~225.562 GHz is a blend of eight transitions whose positions are shown. From *Bockelée-Morvan et al.* (2000).

5.4. Symmetric Hydrocarbons

Symmetric hydrocarbons lack a permanent dipole moment and their excited electronic states predissociate, hence only their ro-vibrational bands are observable in cometary comae. Since 1996, CH_4, C_2H_2, and C_2H_6 have been detected in many comets. The overall appearance of the 3.0-μm region, which is particularly rich in emission lines from hydrocarbons and other species, is shown in Fig. 9 for Comet C/1999 H1 (Lee). A tentative detection of C_4H_2 was also obtained in Comet 153P/2002 C1 (Ikeya-Zhang) (*Magee-Sauer et al.,* 2002b). Searches for C_2H_4, C_3H_6, C_3H_8, and C_6H_6 have been negative so far (M. Mumma, personal communication, 2003).

5.4.1. Methane (CH_4). CH_4 was first clearly detected spectroscopically in Comet Hyakutake, through ground-based observations of five lines of the ν_3 band at 3.3 μm (*Mumma et al.,* 1996). Earlier attempts to detect methane are reviewed in *Mumma et al.* (1993). Methane has been detected in every comet searched since then, including Comet Hale-Bopp, C/1999 S4 (LINEAR), C/1999 H1 (Lee) (Figs. 9a,b), C/1999 T1 (McNaught-Hartley), C/2001 A2 (LINEAR), C/2000 WM_1 (LINEAR), and 153P/2002 C1 (Ikeya-Zhang). Its abundance [CH_4/H_2O] ranged from 0.14% to 1.4% in the sample (*Gibb et al.,* 2003) (see section 8).

5.4.2. Acetylene (C_2H_2). C_2H_2 was first detected in Comet Hyakutake, through three lines of its ν_3 band at 3.0 μm (*Brooke et al.,* 1996). The Oort cloud comets sampled up to now are consistent with [C_2H_2/H_2O] = 0.2–0.5% (Table 1), excepting C/1999 S4 (LINEAR) for which the abundance relative to H_2O was significantly lower (<0.12% at the 2σ limit) (*Mumma et al.,* 2001a) (see section 8). The abundance retrieved from *in situ* measurements of 1P/Halley was ~0.3% (*Giotto* NMS) (*Eberhardt,* 1999).

5.4.3. Ethane (C_2H_6). C_2H_6 was first detected in Comet Hyakutake, when emissions in four Q-branches of its ν_7 band (3.35 μm) were measured (*Mumma et al.,* 1996). C_2H_6 has been detected in every comet searched since then (*Mumma et al.,* 2003). Among Oort cloud comets, the abundance is remarkably constant ([C_2H_6/H_2O] ~ 0.6% (Table 1), the sole exception being C/1999 S4 (LINEAR) (*Mumma et al.,* 2001a). The abundance retrieved from *in situ* measurements of Comet Halley was 0.4% (*Giotto* NMS) (*Eberhardt,* 1999). However, C_2H_6 was significantly depleted in 21P/Giacobini-Zinner, the quintessential C_2-depleted Jupiter-family comet (*Mumma et al.,* 2000; *Weaver et al.,* 1999a;

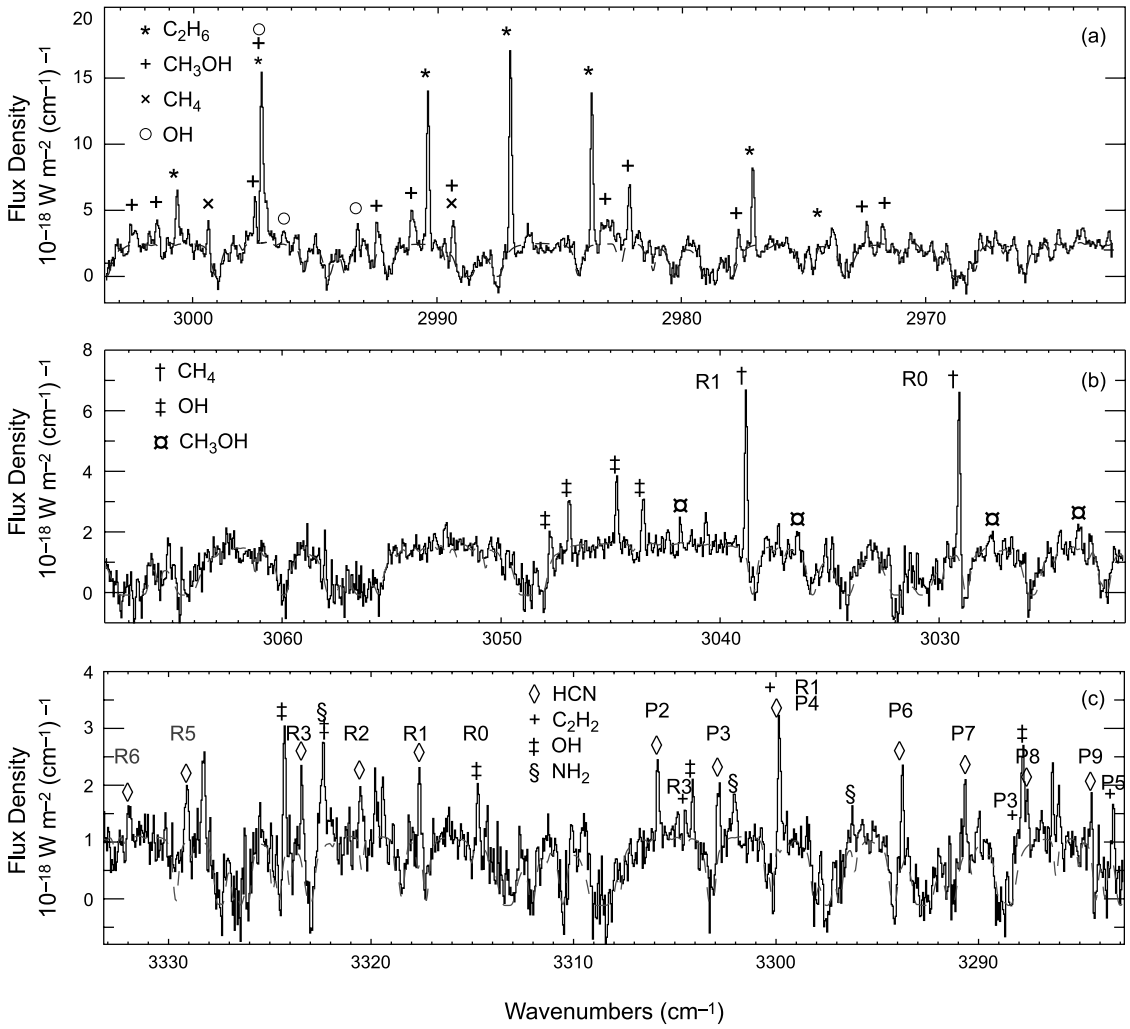

Fig. 9. High-dispersion spectra of Comet C/1999 H1 (Lee) obtained on August 21, 1999 with NIRSPEC at the Keck telescope in the 3-μm region. The dashed line shows a synthetic spectrum of the atmospheric transmittance. Adapted from *Mumma et al.* (2001b).

A'Hearn et al., 1995). The ν_5 band (3.45 μm) of C_2H_6 was detected in Comets Hale-Bopp, Lee, and C/2001 A2 (LINEAR), but it has not yet been quantitatively analyzed (M. Mumma, personal communication, 2003).

5.5. Sulfur-bearing Molecules

5.5.1. CS radical tracing carbon disulfide (CS_2). The CS radical, which is observed at both UV and radio wavelengths (see *Feldman et al.,* 2004) is thought to trace CS_2. The inferred CS_2 abundances range from 0.04% to 0.3% (*Meier and A'Hearn,* 1997). CS_2 has a very short lifetime (~500 s at r = 1 AU), and the spatial brightness profiles of CS measured during the UV observations are consistent with the hypothesis that CS is derived from a short-lived parent.

5.5.2. Hydrogen sulfide (H_2S). Hydrogen sulfide was first detected through its 1_{10}–1_{01} line at 169 GHz at the IRAM 30-m telescope in Comets C/1989 X1 (Austin) and C/1990 K1 (Levy) (*Bockelée-Morvan et al.,* 1991; *Crovisier et al.,* 1991a). It was subsequently observed in several other comets (*Biver et al.,* 2002b), but only through its two millimetric lines at 169 and 217 GHz. The H_2S/H_2O ratio ranges from 0.12% to 1.5%.

Protonated H_2S was identified in ion mass spectra of Comet 1P/Halley, from which a $[H_2S]/[H_2O]$ abundance of 0.4% was derived. This value is within the range of values measured in other comets (*Eberhardt et al.,* 1994).

5.5.3. Sulfur monoxide and dioxide (SO and SO_2). SO and SO_2 have so far been detected only in Comet Hale-Bopp, through several rotational transitions at radio wavelengths (*Lis et al.,* 1999; *Bockelée-Morvan et al.,* 2000) (see Figs. 2 and 8). The 6_5–5_4 line of SO at 219.949 GHz was imaged with IRAM/PdBi, and shows a brightness distribution consistent with a daughter distribution (*Wink et al.,* 1999). It is likely that SO can be fully explained by the

photodissociation of SO_2 (*Bockelée-Morvan et al.,* 2000). Before these detections, *Kim and A'Hearn* (1991) derived upper limits on $Q(SO)/Q(H_2O)$ and $Q(SO_2)/Q(H_2O)$ production rate ratios from the absence of their electronic bands in the UV, which are much lower than those inferred from the radio observations of Comet Hale-Bopp (0.3% and 0.2% for SO and SO_2 respectively): A reappraisal of the g-factors of these bands is certainly necessary.

5.5.4. Carbonyl sulfide (OCS). OCS was first detected through its J(12–11) radio line at 145.947 GHz by *Woodney et al.* (1997) in Comet Hyakutake, and confirmed by several other radio lines in Comet Hale-Bopp (Fig. 8) (*Lis et al.,* 1999; *Bockelée-Morvan et al.,* 2000). Lines of the strong ν_3 band at 4.85 μm (g-factor of 2.6×10^{-3} s^{-1}) were observed by *Dello Russo et al.* (1998) in Comets Hyakutake and Hale-Bopp. In the latter comet, the long-slit infrared observations suggested an extended source for OCS (section 7.2). Inferred $Q(OCS)/Q(H_2O)$ are 0.1% and 0.4% for Comets Hyakutake and Hale-Bopp respectively.

5.5.5. Thioformaldehyde (H_2CS). H_2CS was detected by one rotational line (7_{16}–6_{15} at 244 GHz) in Comet Hale-Bopp with the 12-m radio telescope of the National Radio Astronomy Observatory (NRAO) (*Woodney et al.,* 1999). Its abundance relative to H_2O has been evaluated to 0.05% by *Woodney* (2000).

5.5.6. Disulfur (S_2). The S_2 molecule was discovered during IUE observations of C/1983 H1 (IRAS-Araki-Alcock) when several bands of the $B^3\Sigma_u^- – X^3\Sigma_g^-$ system near 2900 Å were detected (*A'Hearn et al.,* 1983). A reanalysis of those data using improved spectral reduction techniques and revised g-factors (*Budzien and Feldman,* 1992) suggests that the $[S_2/H_2O]$ abundance varied from 0.007% to 0.25% during the course of the observations.

The most common form of solid sulfur is S_8, and the discovery of S_2 in a comet was the first detection of this unusual molecule in any astronomical object. The lifetime of S_2 is very short (a few hundred seconds at r = 1 AU), which means that exceptional spatial resolution (roughly a few hundred kilometers at the comet) is generally required to detect it. Thanks to the close approach to Earth of C/1996 B2 (Hyakutake) and the high spatial resolution available from HST, S_2 has now been detected in four other comets, with $[S_2/H_2O]$ abundances in the range 0.001–0.005% (Table 1). Thus, whatever its origin, S_2 seems to be ubiquitous in comets, at least the long-period ones, although its abundance apparently varies over a large range. Note, however, that the derived S_2 abundances are usually strongly dependent on the assumed S_2 lifetime, whose uncertainty could inflate the true abundance variation.

5.5.7. NS radical. NS was detected through the two J(15/2–13/2) e and f radio transitions at the James Clerk Maxwell Telescope (JCMT) by *Irvine et al.* (2000b) in Comet Hale-Bopp. The origin of this molecule is puzzling; NS is a radical that is unlikely to be present in cometary ices, but no plausible parent could be found. Because its spatial distribution and photodissociation rate are unknown, its abundance relative to H_2O $Q(NS)/Q(H_2O)$ is highly uncertain, but estimated to ≥0.02% (*Irvine et al.,* 2000b).

5.6. Nitrogen-bearing Molecules

With an abundance of ~0.5% relative to H_2O, NH_3 is apparently the dominant N-bearing cometary molecule. The abundance of the super volatile molecule N_2 in cometary nuclei, which would constrain the formation conditions of these objects in the solar nebula, is the subject of continuing debate.

5.6.1. N_2. As mentioned in section 3.4, FUSE searches for UV fluorescence from N_2 have been unsuccessful. The upper limit on the $[N_2/H_2O]$ ratio in two long-period comets [C/2001 A2 (LINEAR) and C/2000 WM_1 (LINEAR)] was <0.2%, while the $[N_2/CO]$ ratio in those same two comets was <30% (P. D. Feldman, personal communication, 2003).

Mass spectrometry in Comet Halley has also not been very helpful in constraining the N_2 abundance because of the accidental coincidence in the masses of N_2 and CO (*Eberhardt et al.,* 1987).

The presence of N_2 in comets is indirectly inferred from emissions in the $B^2\Sigma_u^+ – X^2\Sigma_g^+$ First Negative System of the N_2^+ ion near 3910 Å. During observations ranging from early in the twentieth century all the way up to the 1986 apparition of 1P/Halley, detections of this band have been claimed in many comets (e.g., *Wyckoff et al.,* 1991, and discussion in *Cochran et al.,* 2000). N_2 abundances of ~0.02% relative to H_2O have been derived from these observations. However, high-spectral-resolution observations of some recent comets [122P/de Vico, C/1995 O1 (Hale-Bopp), and 153P/2002 C1 (Ikeya-Zhang)] did *not* detect the N_2^+ band (*Cochran et al.,* 2000; *Cochran,* 2002), with upper limits of $\leq 10^{-5}$–10^{-4} on the abundance of N_2 relative to CO. Thus, the reality of the detection of the N_2^+ ion in the low-resolution spectra of comets observed earlier may be questioned, especially considering the severe spectral blending by emissions from CO^+, CO_2^+, CH, and CH^+ bands in this same region, and potential confusion with N_2^+ emissions from airglow and aurora.

5.6.2. Ammonia (NH_3). Ammonia was tentatively detected from its 24-GHz inversion line in Comet C/1983 H1 (IRAS-Araki-Alcock) by *Altenhoff et al.* (1983). Confirmed detections of several inversion lines were obtained in Comets Hyakutake (*Palmer et al.,* 1996) and Hale-Bopp (*Bird et al.,* 1997, 1999; *Hirota et al.,* 1999), from which abundances of ~0.5% were derived (Table 1). An upper limit of 0.2% was measured for Comet 153P/2002 C1 (Ikeya-Zhang) (*Bird et al.,* 2002).

The infrared ν_1 band of NH_3 at 3.00 μm was detected in Comets Hale-Bopp (tentatively) (*Magee-Sauer et al.,* 1999) and 153P/2002 C1 (Ikeya-Zhang) (K. Magee-Sauer et al., personal communication, 2003).

Ammonia was also indirectly investigated from the bands of its photodissociation products NH and NH_2, which are easily observed in the visible (see *Feldman et al.,* 2004).

From detailed chemical modeling, *Meier et al.* (1994) investigated the relative contributions of NH_3^+ vs. OH^+ and NH_4^+ vs. H_2O^+ at masses 17 and 18 in *Giotto* NMS spectra. They inferred an NH_3 abundance of 1.5% in Comet 1P/Halley, a factor 2–3 times higher than the values measured in Comets Hyakutake and Hale-Bopp.

5.6.3. Hydrogen cyanide (HCN) and hydrogen isocyanide (HNC). HCN was firmly detected in Comet Halley from its J(1–0) line at 88.6 GHz by several teams (*Despois et al.,* 1986; *Schloerb et al.,* 1986, 1987; *Winnberg et al.,* 1987). It is now one of the easiest parent molecules to observe from the ground and can serve as a proxy for monitoring gas production evolution. It is also found to be in remarkably constant ratio with H_2O production (~0.1% according to radio measurements, see section 8), so that it can be used to evaluate relative molecular abundances (*Biver et al.,* 2002b).

HCN is also observed in the infrared through its ν_3 band at 3.0 μm (*Brooke et al.,* 1996; *Magee-Sauer et al.,* 1999; *Mumma et al.,* 2001b). The spectrum of Comet Lee in Fig. 9c shows many ro-vibrational lines of HCN. For some comets, there is a factor of two discrepancy between infrared and radio determinations of the HCN abundance relative to H_2O (Table 1).

HNC, an isomeric form of HCN that is unstable in usual laboratory conditions, was first detected from its J(4–3) line at 363 GHz in Comet Hyakutake (*Irvine et al.,* 1996). It was then observed in Hale-Bopp by several groups (*Irvine et al.,* 1998; *Biver et al.,* 2002a; *Hirota et al.,* 1999) and in several other comets (*Biver et al.,* 2002b; *Irvine et al.,* 2003). The origin of HNC is subject to debate. For Comet Hale-Bopp, an increase of the HNC/HCN ratio (from 0.03 to 0.15) was observed when the comet approached the Sun and became more active; this was interpreted as a clue to chemical conversion of HCN to HNC in the coma, which becomes more efficient in a denser coma (*Irvine et al.,* 1998). However, high HNC/HCN ratios were also observed in Comets Hyakutake, C/1999 H1 (Lee), and C/2001 A2 (LINEAR), which were only moderately productive (Table 1). The HNC/HCN ratio seems to be rather inversely correlated with r (*Biver et al.,* 2002b; *Irvine et al.,* 2003), which would favor a production due to thermo-desorption from heated grains.

5.6.4. Methyl cyanide (HC_3N) and cyanoacetylene (CH_3CN). Two other nitriles are observed in comets. CH_3CN was first detected in Comet Hyakutake with the IRAM interferometer in single-dish mode through a series of rotational lines at 92 GHz (*Dutrey et al.,* 1996). HC_3N was first detected in Comet Hale-Bopp through several rotational lines (*Lis et al.,* 1999; *Bockelée-Morvan et al.,* 2000 (see Fig. 2). These two molecules are 10 times less abundant than HCN (Table 1).

5.6.5. Isocyanic acid (HNCO). A single radio line of HNCO was observed at the Caltech Submillimeter Observatory (CSO) in Comet Hyakutake (*Lis et al.,* 1997). Confirmation was obtained by detection of several rotational lines in Comet Hale-Bopp (Fig. 8) (*Lis et al.,* 1999; *Bockelée-Morvan et al.,* 2000). It was also observed in 153P/2002 C1 (Ikeya-Zhang) (N. Biver et al., personal communication, 2002). Its abundance relative to H_2O is in the range 0.04–0.1%.

5.6.6. Formamide (NH_2CHO). NH_2CHO was detected by several radio lines in Comet Hale-Bopp at CSO and IRAM and the inferred abundance is 0.015% (Fig. 8) (*Lis et al.,* 1999; *Bockelée-Morvan et al.,* 2000).

5.7. Noble Gases

The noble gases (He, Ne, Ar, Kr, and Xe, in order of increasing atomic mass and decreasing volatility) are both chemically inert and highly volatile. Thus, their abundances in cometary nuclei are especially diagnostic of the comet's thermal history. However, remote observations of the noble gases are difficult because their resonance transitions lie in the far-UV spectral region ($\lambda \leq 1200$ Å), which is accessible only from space and is outside the wavelength range covered by the HST and the Chandra X-ray observatory. Searches for several noble gases (He, Ne, and Ar) have been attempted by sounding rockets (*Green et al.,* 1991; *Stern et al.,* 1992, 2000), the Hopkins Ultraviolet Telescope (*Feldman et al.,* 1991), the Extreme Ultraviolet Explorer (EUVE) (*Krasnopolsky et al.,* 1997), the Solar and Heliospheric Observatory (SOHO) (*Raymond et al.,* 2002), and FUSE (*Weaver et al.,* 2002a), but there has not yet been a convincing detection of any noble gas sublimating from a cometary nucleus.

5.7.1. Helium. Helium is the lightest and most volatile of the noble gases, and significant amounts could be frozen in cometary nuclei only if the equilibrium temperature never rose above a few kelvins. For this reason, the detection of emission in the He resonance line at 584 Å during EUVE observations of Comet Hale-Bopp was not interpreted in terms of the production of He atoms sublimating from the nucleus (*Krasnopolsky et al.,* 1997). Rather, the emission could be fully explained by invoking charge exchange between He II solar wind ions and cometary neutral species, which produces He in an excited state that can then relax radiatively [i.e., the same excitation mechanism responsible for cometary X-rays; see *Lisse et al.* (2004)]. Thus, observations of He emission from comets do not shed any light on the thermal history of cometary nuclei, but they can be used as probes of the solar wind conditions and of the interaction between cometary neutrals and the solar wind.

5.7.2. Neon. Neon is also highly volatile, with a sublimation temperature of ~10 K under solar nebula conditions. Fortuitously, the Ne resonance line at 630 Å overlaps the strong solar O V line, which boosts the Ne g-factor upward by a factor of ~100 relative to what it would be if only the solar continuum was available for the excitation. A sensitive search for this Ne line in Comet Hale-Bopp with EUVE resulted in an upper limit on the [Ne/O] abundance that was depleted by a factor of ~25 relative to the solar value in the ice phase, and by a factor of ~200 in total (gas + dust) (*Krasnopolsky et al.,* 1997). An even more sensitive upper limit was obtained for Comet Hyakutake; [Ne/O] was depleted by

a factor of 700 in ice and by more than 2600 in total relative to the solar value (*Krasnopolsky and Mumma,* 2001).

5.7.3. Argon. There was a claimed detection of the two principal resonance lines of Ar at $\lambda = 1048.22$ and 1066.66 Å during a sounding rocket observation of Comet Hale-Bopp in 1997 (*Stern et al.,* 2000). The deduced [Ar/O] ratio was rather high, 1.8 ± 0.96 times the solar value of $[Ar/O]_\odot = (46 \pm 8) \times 10^{-4}$, but the CO abundance was also high (≈12%) (*DiSanti et al.,* 2001), indicating that Comet Hale-Bopp retained highly volatile material. Recent high-spectral-resolution observations of comets with FUSE (*Weaver et al.,* 2002a) demonstrate that there are other lines that can be confused with Ar emission in low-resolution spectra like those of *Stern et al.* (2000), which makes the Ar detection in Comet Hale-Bopp questionable.

Sensitive searches for Ar have been made with FUSE in two long-period comets, C/2000 WM_1 (LINEAR) and C/2001 A2 (LINEAR) (*Weaver et al.,* 2002a). Argon was not detected in either comet, and the [Ar/O] abundance was depleted by at least a factor of 10 (5σ result) relative to the solar value. These large Ar depletions may not be surprising because the abundance of CO, which has comparable volatility to Ar, was also very low in these comets (below 1%). The upper limit on [Ar/O] for the only CO-rich comet observed by FUSE so far, C/1999 T1 (McNaught-Hartley) with $[CO/H_2O] \approx 13\%$, was not very constraining, no larger than the solar abundance at the 5σ level.

Given the string of null results discussed above, information on the noble gas content in cometary nuclei may not be obtained until a mass spectrometer makes sensitive *in situ* measurements.

5.8. Other Molecules and Upper Limits

Polycyclic aromatic hydrocarbons (PAHs) are thought to be an important constituent of interstellar matter, responsible for the ubiquitous emission bands near 3.28, 7.6, and 11.9 μm (C–H stretching, C–C stretching, and C–H bending modes respectively). Are PAHs also present in comets? An emission band near 3.28 μm has been observed in some comets (e.g., *Davies et al.,* 1991; *Bockelée-Morvan et al.,* 1995) (see Fig. 6) and tentatively attributed to PAHs in the gas phase, although other species, such as CH_4 and OH prompt emission are also contributing at this wavelength. This PAH band was not observed in Comet Hale-Bopp, either from the ground or with ISO, but the ISO spectra were obtained at relatively large heliocentric distances ($r > 2.7$ AU) where the PAHs may not be emitting efficiently. *Moreels et al.* (1993) claimed to detect phenanthrene ($C_{14}H_{10}$) in the near-UV spectrum of 1P/Halley measured by the three-channel spectrometer on *Vega*, but this result has not been confirmed by any other observation. Perhaps the best suggestion for cometary PAHs comes from the identification of napthalene, phenanthrene, and other PAHs in laser ablation studies of dust collected in the terrestrial stratosphere that is thought to be of cometary origin (*Clemett et al.,* 1993). In summary, the presence and precise composition of PAHs in cometary nuclei remain open issues requiring further investigation. Some problems that still need to be addressed more rigorously include the excitation mechanism for PAHs, which is thought to be dominated by electronic pumping in the UV followed by intermode conversion to excitation of the numerous PAH vibrational modes; how PAHs are released from cometary refractories to the gas phase; and the lifetime of PAHs in cometary comae (*Joblin et al.,* 1997).

In addition to the detected molecules discussed above and listed in Table 1, upper limits have been set for many other species from dedicated or serendipitous searches at radio and IR wavelengths. A selection of upper limits obtained from radio observations of Comet Hale-Bopp (*Crovisier et al.,* 2004a) is listed in Table 2.

Numerous unidentified features have been detected in cometary spectra. This indicates that new cometary species are still to be identified, pending further theoretical spectroscopic investigations and laboratory measurements. Unidentified lines observed in the visible and UV domains are presumably due to atoms, radicals, or ions (cf. *Feldman et al.,* 2004). Likely, many of these unidentified lines are due to already known cometary species (e.g., C_2, NH_2, …).

In the IR, several unidentified bands have been noted for a long time. This is the case for the 2.44-μm band (*Johnson et al.,* 1983) and for the 3.3–3.5-μm broad band, which can be only partly attributed to C_2H_6 and CH_3OH (see discussion in section 5.3.1). We have strong indications that the 3.4–3.5-μm excess emission shown in Fig. 6 mainly arises from gas-phase fluorescence and not from refractory organics (*Bockelée-Morvan et al.,* 1995). Recently, many unidentified lines have been detected in IRTF/CSHELL and Keck/NIRSPEC high-resolution spectra (e.g., *Magee-Sauer et al.,* 1999; *Mumma et al.,* 2001b). Some of these latter lines could be due to CH_3OH, whose IR spectrum is still poorly understood. Considering that the IR spectra of simple, stable molecules are well known, we could conclude that the unidentified lines are probably due to radicals or to more complex molecules. A few unidentified lines have also been noted in the radio domain, but they were observed with limited signal-to-noise ratio.

6. HELIOCENTRIC EVOLUTION OF PRODUCTION RATES

Extensive studies of the evolution of the outgassing of many comets as a function of heliocentric distance are available from the observation of daughter species [e.g., *Schleicher et al.* (1998) for 1P/Halley, *Rauer et al.* (2003) for Hale-Bopp]. Spectroscopic observations of parent molecules, however, were generally conducted during the most active phase of the comets (i.e., near perihelion), when the signals received from Earth are expected to be the strongest. Monitoring along comet orbit was only possible for a few bright comets, such as Comet Halley [HCN at $r = 0.6$–1.8 AU (*Schloerb et al.,* 1987)], Hyakutake [HCN, CH_3OH, CO, H_2CO, H_2S at $r = 0.24$–1.9 AU (*Biver et al.,* 1999a)],

and C/1999 H1 (Lee) [H_2O, HCN, CH_3OH, H_2CO at r < 1.7 AU (*Biver et al.,* 2000; *Chiu et al.,* 2001)]. The early discovery at r = 7 AU of Comet Hale-Bopp and its exceptional intrinsic activity [$Q(H_2O) = 10^{31}$ molecules s^{-1} at perihelion] provided the first opportunity to follow the evolution of the production rates of a number of molecules over a much larger heliocentric range. Figure 7 shows the result of a monitoring performed at radio wavelengths (*Biver et al.,* 2002a) during which many molecules were detected up to r = 4–5 AU, and up to 14 AU in the case of CO. Long-slit spectroscopy in the infrared covered the 0.9–4.1-AU range for CO, the 0.9–4-AU range for C_2H_6, and the 0.9–1.5-AU range for H_2O (*DiSanti et al.,* 2001; *Dello Russo et al.,* 2000, 2001).

Gas production curves are almost the only observational tools we have to obtain informations regarding the nature and physical state of cometary ices, and their thermal properties and sublimation mechanisms. A review of the various processes involved in cometary activity, and of the mathematical models developed so far, is presented by *Prialnik et al.* (2004). Gas production curves also complement usefully visual light curves for the study of seasonal effects, dust mantling, etc. (see *Meech and Svoreň,* 2004). A fundamental question that arises and can be addressed observationally from gas production curves is to which extent production rate ratios reflect the bulk composition inside the nucleus. Both numerical simulations and laboratory experiments show that the link is not simple, at least for the most volatile species.

The monitoring performed in Comet Hale-Bopp showed that the coma composition changed with heliocentric distance. CO was the main escaping gas at large r (Fig. 7). The H_2O production rate surpassed that of CO for r < 3 AU. *Capria et al.* (2000) showed that the heliocentric behavior of CO production (roughly in r^{-2} from r = 0.9 to 14 AU) can be explained if CO is present in the nucleus both as pure ice and as trapped gas in amorphous H_2O ice that would be immediately below the surface. This trapped gas is released during the amorphous to crystalline phase transition. In contrast, models considering only the sublimation of pure CO ice fail in reproducing the observed heliocentric dependence.

As seen in Fig. 7, distinct trends are observed among the various molecules. As already discussed, the steep production curves of HNC and H_2CO are likely related to an extended production in the coma (see sections 5.3.2 and 5.6.3). Steep production curves when compared to, e.g., HCN are also observed for CS and OCS (*Woodney,* 2000; *Biver et al.,* 2002a). A pre-/postperihelion asymmetry is also apparent for all molecules.

7. SPATIAL DISTRIBUTION OF PARENT MOLECULES AND EXTENDED SOURCES

The study of the spatial distribution of parent molecules provides clues on the distribution of the outgassing at the surface of the nucleus and on gas dynamics processes occurring in the coma (see *Crifo et al.,* 2004). However, data acquired so far provide limited information due to the lack of spatial coverage and resolution. Radio and long-slit IR spectra provide numerous examples of anisotropic distributions with day/night asymmetries, which will not be discussed here. Rather, we will focus on studies of the radial distribution of molecular species in the coma. Some species can be released directly from the nucleus, and also can be produced in the coma from other precursors. The former source is said to be direct (or native), while the latter is said to be extended (or distributed). The native and extended sources exhibit different radial distributions, and can be recognized in this way.

7.1. Radial Distribution from *In Situ* Measurements

The discovery of extended sources of molecules in the coma was one of the highlights of the space investigation of 1P/Halley. The best examples were for CO (*Eberhardt et al.,* 1987) and H_2CO (*Meier et al.,* 1993). Their densities measured by NMS along the path of the *Giotto* spacecraft do not match those expected for a parent molecule. Only one-third (~3.5% relative to H_2O) of the total CO was released directly from the nucleus, the remainder (~7.5%) being produced from an extended source in the coma (*Eberhardt et al.,* 1987; *Eberhardt,* 1999). H_2CO in Comet Halley was produced mainly, and perhaps totally, from an extended source (*Meier et al.,* 1993). The region containing the extended sources extended to ~10^4 km from the nucleus. *Meier et al.* (1993) estimated the scalelength of the parent source of H_2CO to be 1.2 times the photodissociative scalelength of H_2CO that corresponds to ~5000 km. According to *Eberhardt* (1999), there is also indication of a second extended source of H_2CO with a much longer scalelength. These discoveries sparked keen interest in identifying the nature of the extended sources.

Proposed sources for extended H_2CO focus on the decomposition of (native) polymerized H_2CO (*Meier et al.,* 1993), possibly polyoxymethylene (POM) (*Mitchell et al.,* 1987, 1989; *Huebner,* 1987). Recent laboratory work demonstrates that adequate monomeric H_2CO can be produced by thermal decomposition of POM, if cometary grains are 4% POM by mass in Comet Halley (*Cottin et al.,* 2004).

Photolysis of monomeric H_2CO was suggested as a significant source for extended CO in 1P/Halley. According to *Meier et al.* (1993), the photodissociation of H_2CO provides about two-thirds of the extended CO source. According to *Eberhardt* (1999), H_2CO could even fully account for the extended CO source after a reanalysis of the data. In contrast, in Comet Hale-Bopp, H_2CO was found to be only a minor contributor to extended CO as its production rate was much below that of CO extended production (section 7.2.1). Carbon suboxide (C_3O_2) was suggested as a source of CO (*Huntress et al.,* 1991), but the upper limit derived from *Vega* IKS spectra (C_3O_2 < 0.1%) (*Crovisier et al.,* 1991b) was well below the minimum value (7.5%) required to produce the amount of extended CO inferred

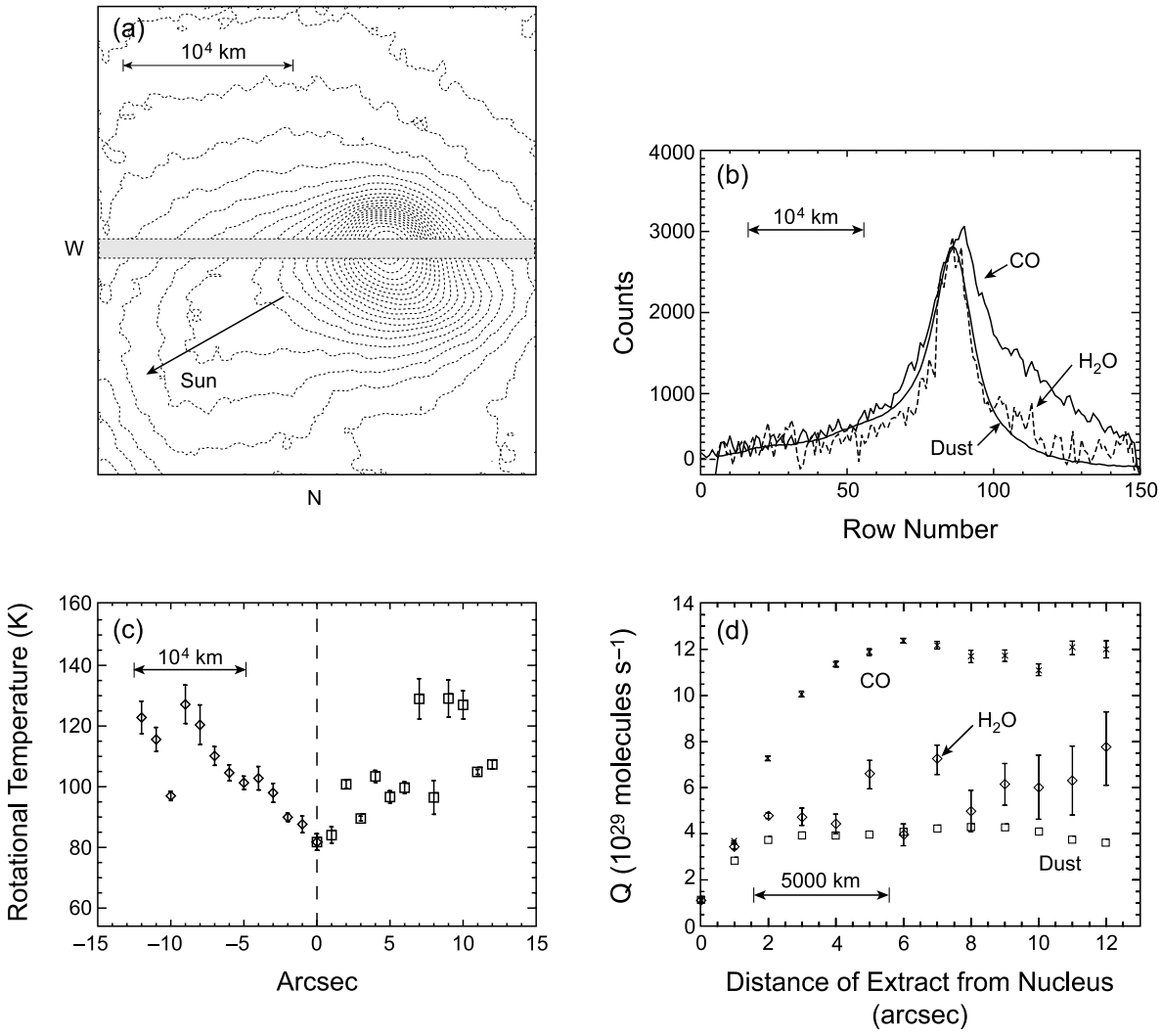

Fig. 10. Observations of Comet Hale-Bopp with IRTF/CSHELL. **(a)** Image of thermal continuum at 3.5 μm ($\lambda/\delta\lambda = 70$). The east-west slit is indicated. **(b)** Spatial profiles of CO, H_2O, and dust along the slit. **(c)** Rotational temperatures for CO along the slit. **(d)** Symmetric Q-curves showing the rise to terminal values. From *DiSanti et al.* (2001).

from the *Giotto* observations. An alternative view, that *Giotto* flew through a jet enriched in CO, was proposed by *Greenberg and Li* (1998) to interpret the NMS observations.

7.2. Radial Distribution from Long-Slit Spectroscopy

7.2.1. Infrared results. When a molecule is released directly from the nucleus, its column density is expected to vary, in first approximation (i.e., Haser model and $\rho \ll v\tau$), as ρ^{-1}, where ρ is the distance between the line of sight and the nucleus (i.e., the impact parameter). If an extended source is also present, the variation of column density with r is much flatter. Under favorable circumstances, this difference can be used to extract the two sources separately. In Comet Hale-Bopp, extended sources were identified for OCS (*Dello Russo et al.,* 1998) and CO (*Weaver et al.,* 1999b; *DiSanti et al.,* 1999, 2001; *Brooke et al.,* 2003), although the ratio of native to extended source production rates for CO remains controversial. In contrast, the column density profiles for H_2O (*Weaver et al.,* 1999b; *Dello Russo et al.,* 2000; *Brooke et al.,* 2003), C_2H_6 (*Weaver et al.,* 1999b; *Dello Russo et al.,* 2001; *Brooke et al.,* 2003), CH_4 (*Weaver et al.,* 1999b; *Brooke et al.,* 2003), and HCN (*Magee-Sauer et al.,* 1999) were consistent with release solely from the nucleus.

The technique is illustrated for Comet Hale-Bopp in Fig. 10 from *DiSanti et al.* (2001). An image of the thermal continuum near 3.5 μm ($\lambda/\delta\lambda \sim 70$) reveals dust enhancements to the northeast and northwest (sunward) of the nucleus (Fig. 10a). High-dispersion spectra were measured with the slit positioned as shown. The intensity profiles

measured along the slit show that CO is extended to the east while H_2O is symmetric about the nucleus and the dust is extended to the west (Fig. 10b).

To extract the contribution of the native and extended CO sources, *DiSanti et al.* (2001) developed the method of Q-curves, as shown in Fig. 10d. The intensities measured at symmetric positions along the slit are first averaged to minimize the effects of outflow asymmetry. An apparent production rate can be then derived from the intensity measured at a specific location using equation (11) and the formula that links the column density to the production rate under the idealized assumption of spherical outflow at constant velocity. The resulting Q-curve (Fig. 10d) rises from the nucleocentric value to a terminal value that is taken to represent the *total* production rate for the species. The nucleus-centered value is always too low, owing to slit losses induced by seeing, drift, guiding error, and other observing factors, but the terminal value is reached quickly for molecules released directly from the nucleus (e.g., H_2O, C_2H_6, CH_4, dust). Molecules having an extended source rise more slowly to the terminal value (e.g., CO, OCS) (compare Q-curves for CO, H_2O, and dust; Fig. 10d).

It was estimated that ~70% of OCS was produced from an extended source in Comet Hale-Bopp near perihelion (*Dello Russo et al.,* 1998). At large heliocentric distance (4.1 AU < r < 2 AU), the spatial profile of CO was consistent with its release solely from the nucleus. However, within 2 AU an *extended* source was activated, and it supplied at least half the total CO released thereafter (0.9 AU < r < 1.5 AU) (*DiSanti et al.,* 2001); using a different approach involving explicit modeling of both parent and daughter spatial distributions, *Brooke et al.* (2003) estimated that ~90% of the observed CO was derived from the extended source at r = 1 AU, in apparent contradiction with the conclusions of *DiSanti et al.* (2001). The abrupt onset and constant fractional production of the extended source thereafter suggest a thermal threshold for release from small CHON grains, rather than photolysis of a precursor volatile. Monomeric H_2CO was at most a minor contributor to extended CO in Comet Hale-Bopp. Carbon dioxide is admittedly a significant source of CO. However, it cannot explain the extended CO source observed in the IR, which has a scalelength much smaller than the CO_2 photodissociation scalelength. In Comet Hyakutake, CO was abundant and it was released almost entirely from the nucleus (*DiSanti et al.,* 2003).

7.2.2. Ultraviolet results. The advent of the long-slit capability of the Space Telescope Imaging Spectrograph (STIS) on HST now permits extremely high-spatial resolution studies of CO and S_2. However, the small g-factors for the CO emissions makes this approach feasible only for the brightest comets. While the g-factors are much larger for S_2, its abundance is so low that poor signal-to-noise is a problem in this case as well. Nevertheless, accurate spatial brightness profiles for S_2 were recently obtained in 153P/2002 C1 (Ikeya-Zhang) and indicate that S_2 probably originates in the nucleus but may have a lifetime that is significantly longer than the theoretical value (*Weaver et al.,* 2002b).

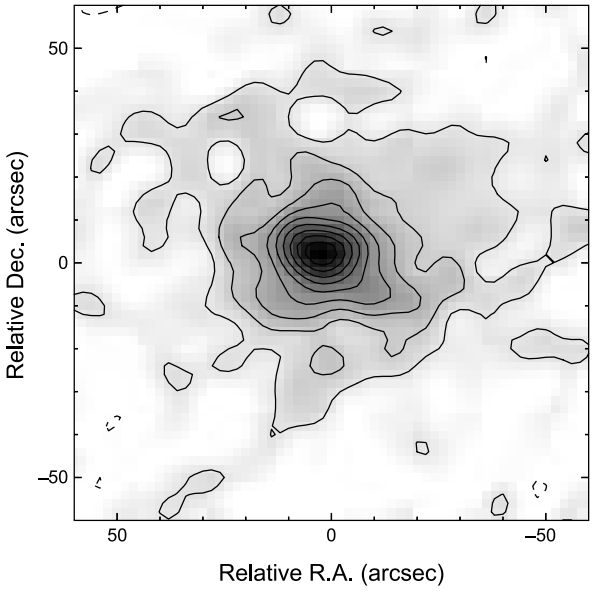

Fig. 11. Mosaicked image of HCN J(1–0) main hyperfine component (F = 2–1) obtained on April 6, 1997, for Comet Hale-Bopp with the BIMA array. Contour interval: 0.23 K averaged over 3.5 km s^{-1}. The angular resolution is 10". From *Wright et al.* (1998).

7.3. Millimeter Wave Mapping/Interferometry

Mapping of rotational emission lines was only attempted in a few comets. Most investigations were performed in Comets Hyakutake and Hale-Bopp, due to their exceptional brightnesses. Focal plane arrays and on-the-fly mapping (which consists in moving the telescope beam across the source at a constant velocity) provided extended coverage of the molecular emissions with single-dish telescopes, although with limited spatial resolution (10" at most) [(e.g., *Lovell* (1999) using QUARRY at the Five College Radio Astronomy Observatory (FCRAO)]. Large maps using conventional techniques were also obtained (e.g. *Hirota et al.* (1999) at the Nobeyama 45-m telescope; *Biver et al.* (1999a) at JCMT). Interferometry techniques have been successfully used for the first time, and provided angular resolutions up to 2". Numerous observations were performed in Comet Hale-Bopp with the IRAM Plateau de Bure interferometer, the array of the Berkeley-Illinois-Maryland Association (BIMA), and the Owens Valley Radio Observatory (OVRO). Interferometric maps of rotational lines of CO, HCN (e.g., Fig. 11), H_2S, CS, SO, H_2CO, HNC, DCN, HDO, and CH_3OH were obtained (*Blake et al.,* 1999; *Veal et al.,* 2000; *Wink et al.,* 1999; *Wright et al.,* 1998; *Woodney et al.,* 2002). In contrast to other spectral domains, additional information on the spatial distribution along the line of sight can be extracted from the radio maps by analyzing the line shapes.

Maps of Comet Hale-Bopp show the presence of gaseous jets. The images obtained by *Blake et al.* (1999) with OVRO show HNC, DCN, and HDO emissions offset by a few arcseconds with respect to the dust continuum emission, interpreted as due to jets enriched in these molecules. No such offsets were observed for other species mapped with millimeter interferometry. *Veal et al.* (2000) observed structures in HCN J(1–0) maps obtained with BIMA, which varied and disappeared on timescales ~2 h. These variations may trace rotating HCN jets, as observed for CO. Indeed, a sinusoidal temporal variation in the spectral shift of the CO J(2–1) line was observed at IRAM/PdBi (*Henry et al.,* 2002; *Henry,* 2003). Both the period of this sinusoid, which is consistent with the nucleus rotation period, and the time modulation of the signals received by the antenna pairs, suggest the existence of a CO spiraling jet. From the maps of Comets Hyakutake and Hale-Bopp (*Biver et al.,* 1999a; *Wink et al.,* 1999), H_2CO clearly appears extended with a parent scalelength consistent with that derived for 1P/Halley from the *in situ* measurements. Coarse radio mapping in C/1989 X1 (Austin) gave similar results (*Colom et al.,* 1992). In contrast, the HCN and H_2S maps of Comet Hale-Bopp (*Wink et al.,* 1999; *Wright et al.,* 1998) are consistent with parent molecule distributions. As discussed in section 5.5.3, the interferometric observations of SO show that this species does not follow a parent density distribution, and suggest the photolysis of SO_2 as the main source of SO (*Wink et al.,* 1999).

Other observational clues for extended sources obtained by radio observations concern distant comets. *Gunnarsson et al.* (2002) mapped the CO J(2–1) line in Comet 29P/Schwassmann-Wachmann 1 with the SEST telescope. They concluded that there was a large (~70%) contribution of CO coming from an extended source, likely sublimating icy grains. No such imaging was performed in Comet Hale-Bopp when far from the Sun. However, the CO line shapes of Comet Hale-Bopp at large r resemble those of 29P/Schwassmann-Wachmann 1, which led *Gunnarsson et al.* (2003) to suggest that sublimating grains were also contributing to the CO production in Comet Hale-Bopp when at $r > 4$ AU. These line profiles are asymmetric, and characterized by a pronounced peak on the blue wing of the line, and a redshifted part of lower intensity. This blue peak would correspond to nuclear production toward the Sun, while the redshifted component is the red part of a symmetric profile due to the secondary source. Much more symmetric radio lines were observed for CH_3OH, H_2CO, and OH at $r > 3.5$ AU (*Biver et al.,* 1997; *Womack et al.,* 1997). These results are consistent with a relative contribution of the icy grains vs. nucleus outgassing being more important for CH_3OH, H_2CO, and H_2O than for CO. This may be not surprising given the lower volatilities of CH_3OH, H_2CO, and H_2O ices compared to CO ice.

Snyder et al. (2001) used the maps of HCN J(1–0) and CS J(2–1) obtained in Comet Hale-Bopp with the BIMA array to measure the photodissociation rates of these molecules. That of HCN was found consistent with theoretical predictions, while a photodissociation rate 10 times larger than the commonly accepted value is suggested for CS.

8. MOLECULAR ABUNDANCES AND CHEMICAL DIVERSITY AMONG COMETS

According to current theories, comet formation in the solar nebula extended over a wide range of heliocentric distances for both Oort cloud comets [also called nearly isotropic comets (*Dones et al.,* 2004)] and Jupiter-family comets [now recognized as a subclass of the ecliptic comets (*Duncan et al.,* 2004; *Morbidelli and Brown,* 2004)], which suggests that comets could display diversity in their chemical composition depending on the local temperature and nebular composition where they formed. If there was significant mixing of nebular material across large ranges in heliocentric distance, even individual cometary nuclei could exhibit chemical inhomogeneity.

Chemical diversity among comets is indeed observed for both parent volatiles and daughter species. From a study of radicals (OH, CN, C_2, C_3, NH) in 85 comets, *A'Hearn et al.* (1995) proposed the existence of two classes of comets, depending on their C_2/CN ratio: "typical" comets and "C_2-depleted" comets. They found that about one-half the Jupiter-family comets (JFCs) were C_2-depleted, but the fraction of C-depleted nearly isotropic comets was much smaller. The meaning of this depletion is clouded by two factors. First, the relative production of C_2 and CN from several possible gas and dust precursors is not known. Second, the present volatile composition of a JFC may not reflect its original volatile composition. Jupiter-family comets typically have low-inclination, prograde orbits with periods less than ~20 years, and they are subjected to much greater insolation than the nearly isotropic comets. Thus, some JFCs may have experienced thermal fractionation while in their present orbits.

Surveys of parent volatile abundances show strong evidence for chemical diversity among comets (Fig. 12 and Table 1). Among the Oort cloud comets (OCCs), the native CO abundance varies by a factor of ~40 (0.4–17%) relative to H_2O. The abundance of extended CO varies by a similar amount, but the two sources are not correlated. The comet-to-comet differences in native CO are presumably attributable to intrinsic variation in the amount of CO ice frozen into cometary nuclei. The CO_2 abundance varied by a factor of five (2.5–12%) among five comets (*Feldman et al.,* 1997), although this conclusion rests on the assumption that the observed CO Cameron band emission was due solely to the photodissociation of CO_2. Infrared investigations of CO_2 in three comets indicate CO_2/H_2O variations by at least a factor of 2.

Infrared observations of hydrocarbons in a handful of comets (*Mumma et al.,* 2003; *Gibb et al.,* 2003) show that the CH_4 abundance varies by a factor of ~10 (0.14–1.4%), apparently without correlation with CO. Thus, one cannot

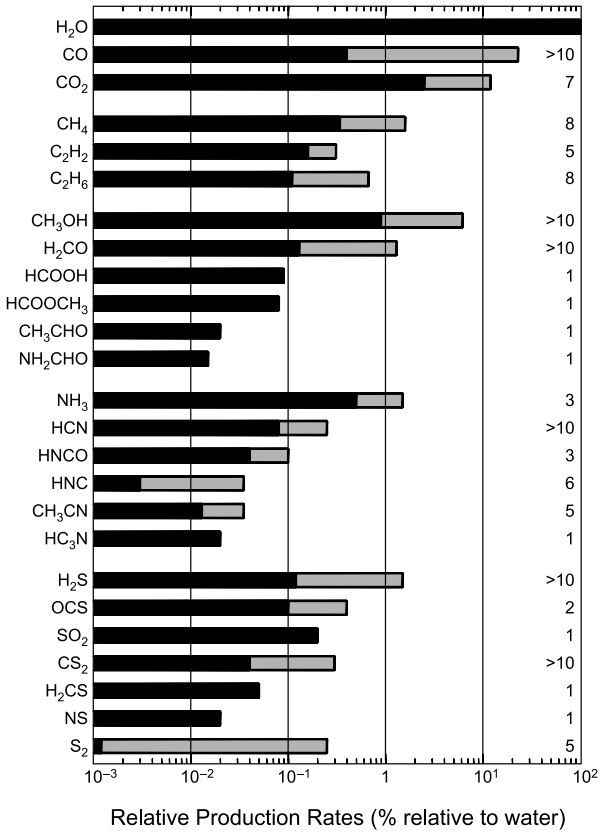

Fig. 12. Abundances relative to water in comets. The range of measured values is shown in the gray portions. The number of comets for which data are available is given in the right. For CO, abundances refer to total CO (native and distributed sources).

define a "typical" abundance for either CO or CH_4. The C_2H_6 abundance shows less diversity, with six OCCs showing ~0.4–0.7% and only C/1999 S4 (LINEAR) differing greatly. In the same group of comets, the C_2H_2 abundance was typically 0.2–0.3%, but it was significantly lower in C/1999 S4. The CH_3OH abundance is ~2% in 14 comets (including all four JFCs sampled) observed in the infrared, but three OCCs had much lower abundances [C/1990 K1 (Levy), C/1996 Q1 (Tabur), and C/1999 S4] and two had much higher abundances [C/1989 X1 (Austin), 109P/Swift-Tuttle].

From radio observations of about 25 comets (including 6 JFCs), *Biver et al.* (2002b) studied the production rates of HCN, HNC, CH_3CN, CH_3OH, H_2CO, CO, CS, and H_2S relative to H_2O. Hydrogen cyanide is the best-studied molecule. In contrast to other species, the distribution of the HCN/H_2O ratios is strongly peaked, with most comets around 0.1%. Observed in more than 10 comets, CH_3OH, H_2CO, and H_2S show large variations. The distribution of CH_3OH/H_2O ratios follows that measured from infrared spectra. The H_2CO/H_2O abundance ranges from 0.4% to 1.3% in 12 comets, but is significantly lower (≤0.15%) in 21P/Giacobini-Zinner. H_2S/H_2O varies from 0.4% to 1.5% in 10 comets, but is only 0.12% in C/2000 WM_1 (LINEAR). The comets that are abundant in CH_3OH are also abundant in H_2CO. No clear correlation is found between the relative abundances and the dynamical origin of the comets, or their dust-to-gas ratios.

From UV observations of the CS radical by IUE and HST of 19 comets (*Meier and A'Hearn,* 1997), the CS_2 abundance varies from 0.04% to 0.3%.

Perhaps one should not be surprised to find significant chemical diversity among even a small sample of nearly isotropic comets because, as stated earlier, the comets from the Oort cloud were probably formed over a large range of heliocentric distances. The most recent dynamical models suggest that comets now in the Oort cloud were contributed in roughly equal numbers by each giant planet and the Kuiper belt (*Dones et al.,* 2004). The chemical diversity found to date suggests that comets from various regions of the protoplanetary disk are present in today's Oort cloud and can provide a window on this crucial period in solar system development. However, many more comets must be sampled and additional parent molecules measured to establish overall taxonomic classes of comets from their chemistry and related parameters.

9. ISOTOPIC COMPOSITION

Isotopic ratios are an important diagnostic of the physical conditions that prevailed during the formation of cometary volatiles, as well as isotopic exchange and mixing processes that may have occurred in the solar nebula before their incorporation into comets. Since most detections of parent molecules postdate 1985, it is not surprising that the detection of their isotopomers is rare. We summarize most of the measurements in Table 3.

The first measurements of the D/H ratio in H_2O were obtained in Comet Halley from mass-resolved ion-spectra of H_3O^+ acquired by the IMS (*Balsiger et al.,* 1995) and NMS (*Eberhardt et al.,* 1995) instruments onboard *Giotto*. These independent data provided precise D/H values, which combined give a D/H value of $\sim 3 \times 10^{-4}$. Thanks to the availability of sensitive groundbased instrumentation in the submillimeter domain, HDO was detected in Comets Hyakutake (Fig. 13) and Hale-Bopp from its 1_{01}–0_{00} line at 464.925 GHz (*Bockelée-Morvan et al.,* 1998; *Meier et al.,* 1998a). The derived D/H values are in agreement with the determinations in 1P/Halley. *Blake et al.* (1999) reported the interferometric detection of the 2_{11}–2_{12} HDO transition at 241.562 GHz in Comet Hale-Bopp and derived a D/H value one magnitude larger in jets compared to the surrounding coma. A serendipitous detection of the 3_{12}–2_{21} HDO line at 225.897 GHz in Comet Hale-Bopp was also reported by *Crovisier et al.* (2004a).

DCN was detected in Comet Hale-Bopp with the JCMT from its J(5–4) rotational transition at 362.046 GHz (*Meier et al.,* 1998b). The inferred D/H value in HCN is 2.3×10^{-3}, i.e., seven times larger than the value in H_2O. The same value is reported by *Crovisier et al.* (2004a) from a marginal detection of the J(3–2) DCN line at the IRAM 30-m telescope. Interferometric observations of this J(3–2) DCN

TABLE 3. Isotopic ratios in comets.

Ratio	Molecule	Comet	Value	Method*	Reference
D/H	H_2O	Halley	$(3.08^{+0.38}_{-0.53}) \times 10^{-4}$	m.s.†	*Balsiger et al.* (1995)
		Halley	$(3.06 \pm 0.34) \times 10^{-4}$	m.s.†	*Eberhardt et al.* (1995)
		Hyakutake	$(2.9 \pm 1.0) \times 10^{-4}$	r.s.	*Bockelée-Morvan et al.* (1998)
		Hale-Bopp	$(3.3 \pm 0.8) \times 10^{-4}$	r.s.	*Meier et al.* (1998a)
	HCN	Hale-Bopp	$(2.3 \pm 0.4) \times 10^{-3}$	r.s.	*Meier et al.* (1998b)
	H_2CO	Halley	$<2 \times 10^{-2}$	m.s.‡	*Balsiger et al.* (1995)
		Hale-Bopp	$<5 \times 10^{-2}$	r.s.	*Crovisier et al.* (2004a)
	CH_3OH	Halley	$<\sim 1 \times 10^{-2}$	m.s.§	*Eberhardt et al.* (1994)
		Hale-Bopp	$<3 \times 10^{-2}$	r.s.¶	*Crovisier et al.* (2004a)
		Hale-Bopp	$<8 \times 10^{-3}$	r.s.**	*Crovisier et al.* (2004a)
	NH_3	Hyakutake	$<6 \times 10^{-2}$	v.s.††	*Meier et al.* (1998c)
		Hale-Bopp	$<4 \times 10^{-2}$	r.s.‡‡	*Crovisier et al.* (2004a)
	CH_4	153P/2002 C1	$<1 \times 10^{-1}$	i.s.	*Kawakita et al.* (2003)
	H_2S	Hale-Bopp	$<2 \times 10^{-1}$	r.s.	*Crovisier et al.* (2004a)
	CH	Hyakutake	$<3 \times 10^{-2}$	v.s.	*Meier et al.* (1998c)
$^{12}C/^{13}C$	C_2	four comets§§	93 ± 10	v.s.	*Wyckoff et al.* (2000)
	CN	Halley	95 ± 12	v.s.	*Kleine et al.* (1995)
	CN	five comets¶¶	90 ± 10	v.s.	*Wyckoff et al.* (2000)
	CN	Hale-Bopp	165 ± 40	r.s.	*Arpigny et al.* (2003)
	CN	C/2000 WM_1	115 ± 20	r.s.	*Arpigny et al.* (2003)
	HCN	Hyakutake	34 ± 12***	r.s.	*Lis et al.* (1997)
	HCN	Hale-Bopp	111 ± 12	r.s.	*Jewitt et al.* (1997)
	HCN	Hale-Bopp	109 ± 22	r.s.	*Ziurys et al.* (1999)
	HCN	Hale-Bopp	90 ± 15	r.s.	*Lis et al.* (1999)
$^{14}N/^{15}N$	CN	Hale-Bopp	140 ± 35	v.s.	*Arpigny et al.* (2003)
	CN	C/2000 WM_1	140 ± 30	v.s.	*Arpigny et al.* (2003)
	HCN	Hale-Bopp	323 ± 46	r.s.	*Jewitt et al.* (1997)
	HCN	Hale-Bopp	330 ± 98	r.s.	*Ziurys et al.* (1999)
$^{16}O/^{18}O$	H_2O	Halley	518 ± 45	m.s.	*Balsiger et al.* (1995)
	H_2O	Halley	470 ± 40	m.s.	*Eberhardt et al.* (1995)
	H_2O	153P/2002 C1	450 ± 50	r.s.	*Lecacheux et al.* (2003)
$^{32}S/^{34}S$	S^+	Halley	23 ± 6	m.s.	*Altwegg* (1996)
	CS	Hale-Bopp	27 ± 3	r.s.	*Jewitt et al.* (1997)
	H_2S	Hale-Bopp	17 ± 4	r.s.	*Crovisier et al.* (2004a)

* m.s.: mass spectrometry; r.s.: radio spectroscopy; v.s.: visible spectroscopy; i.s.: infrared spectroscopy.
† From H_3O^+.
‡ From $HDCO^+$.
§ CH_2DOH and CH_3OD averaged.
¶ For CH_3OD.
** For CH_2DOH.
†† From NH.
‡‡ From NH_2D.
§§ Mean ratio in C_2 from observations in C/1963 A1 (Ikeya), C/1969 T1 (Tago-Sato-Kosaka), C/1973 E1 (Kohoutek), and C/1975 N1 (Kobayashi-Berger-Milon).
¶¶ Mean ratio in CN from five comets: 1P/Halley, C/1990 K1 (Levy), C/1989 X1 (Austin), C/1989 Q1 (Okazaki-Levy-Rudenko), and C/1995 O1 (Hale-Bopp).
*** Ratio possibly affected by line blending.

line lead to DCN/HCN values in jets, which are again significantly larger than the single-dish value (*Blake et al.,* 1999). We note that these differences in isotopic abundance ratios for different regions of the coma (e.g., in and out of jets) must be confirmed by higher-quality interferometric observations before too much effort is expended interpreting these differences.

Finally, upper limits for several other D-bearing molecules were obtained, mainly by millimeter spectroscopy or visible spectroscopy of daughter species (Table 3). Most of these upper limits exceed a few percent and may be not easily improved from further groundbased observations unless a comet as bright as Comet Hale-Bopp is coming.

The measurements of isotopes other than D in cometary volatiles are limited. In Comet Hale-Bopp, rotational transitions of $HC^{15}N$, $H^{13}CN$, and $C^{34}S$ were detected, leading to isotopic ratios that are compatible with the terrestrial values $^{12}C/^{13}C = 89$, $^{14}N/^{15}N = 270$, and $^{32}S/^{34}S = 24$ (*Jewitt*

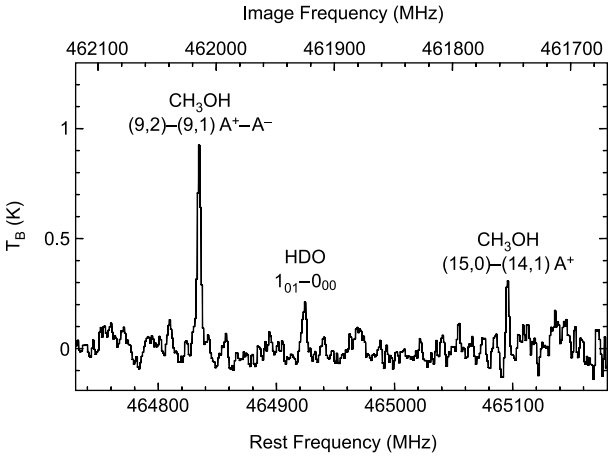

Fig. 13. The 1_{01}–0_{00} line of HDO at 465 GHz observed in Comet C/1996 B2 (Hyakutake) with the CSO (*Bockelée-Morvan et al.,* 1998).

et al., 1997; *Ziurys et al.,* 1999). From a tentative detection of $H_2{}^{34}S$, *Crovisier et al.* (2004a) deduced a $^{32}S/^{34}S$ ratio 30% lower than the terrestrial value. In Comet Hyakutake, *Lis et al.* (1997) inferred a $^{12}C/^{13}C$ ratio in HCN three times lower than the terrestrial value. However, the J(3–2) $H^{13}CN$ line used for this measurement is partly blended with a SO_2 line, so this result is uncertain. Regarding the $^{18}O/^{16}O$ ratio, which has only been measured in H_2O, *in situ* measurements in 1P/Halley are consistent with the terrestrial value of 500 (Table 3). $H_2^{18}O$ has been detected through its fundamental ortho line at 547.7 GHz in Comet 153P/2002 C1 (Ikeya-Zhang) by *Lecacheux et al.* (2003), and the derived $H_2^{18}O/H_2^{16}O$ ratio is consistent with that obtained by mass spectrometry in 1P/Halley.

Lines of ^{13}CN [mainly in the $B^2\Sigma^+$–$X^2\Sigma^+$ v(0–0) system] and $^{13}C^{12}C$ (Swan bands) were identified in visible spectra of several comets. All measurements give a C-isotopic ratio in the CN and C_2 radicals consistent with the terrestrial value [Table 3; see data for individual comets in *Wyckoff et al.* (2000)]. These isotopic ratios may not fully reflect the values in HCN and C_2H_2, as other sources of CN and C_2 radicals are suspected to be present in the coma. *Arpigny et al.* (2003) report anomalous $C^{14}N/C^{15}N$ ratios (~140) in Comets Hale-Bopp and C/2000 WM_1 (LINEAR). This is much less than the ratio $HC^{14}N/HC^{15}N$ = 270 observed in Comet Hale-Bopp, pointing to an additional, still unidentified, source of CN.

10. ORTHO-TO-PARA RATIOS

Molecules with H atoms at symmetrical positions may exist in different nuclear-spin species according to the sum I of the spins of their H atoms. These spin species are called *ortho* (I = 1) and *para* (I = 0) for molecules with two H atoms (e.g., H_2, H_2O, H_2S, H_2CO, …); A and E for molecules with three H atoms (e.g., NH_3 or CH_3OH); A, E, and F for molecules with four H atoms (e.g., CH_4); and so forth. Conversions among different species in the gas phase by radiative transitions or by collisions are strictly forbidden. Conversions are presumably very slow in the solid phase as well, although various proton-exchange mechanisms do exist in that case.

The ortho-to-para population ratio (OPR) can be evaluated from the rotational distribution of the molecules. When there is equilibrium at a temperature T

$$\mathrm{OPR} = \frac{(2I_o + 1)\sum_{\text{o levels}} (2J + 1)\exp\left(-\frac{E}{kT}\right)}{(2I_p + 1)\sum_{\text{p levels}} (2J + 1)\exp\left(-\frac{E}{kT}\right)} \qquad (16)$$

where o and p refer to the ortho and para rotational levels. J and E are the rotational quantum number and energy of the levels respectively. For high temperatures, the populations tend to equilibrate to their statistical weights, 2I + 1. Thus, the high-temperature OPR limit is 3 for H_2O, 1 for NH_3, … (see discussions by *Crovisier,* 1984; *Mumma et al.,* 1993).

From observations of the ν_3 band of H_2O with the KAO, *Mumma et al.* (1993) reported an OPR of 2.5 ± 0.1 for 1P/Halley ($T_{spin} \approx 29$ K) and 3.2 ± 0.2 for C/1986 P1 (Wilson) ($T_{spin} > 50$ K). From observations with ISO (Fig. 3), the OPR was 2.45 ± 0.10 for Comet Hale-Bopp and 2.76 ± 0.08 for 103P/Hartley 2 (*Crovisier et al.,* 1997, 1999b), corresponding to T_{spin} = 28 ± 2 K and 36 ± 3 K, respectively.

Kawakita et al. (2001, 2002) measured the OPR of the NH_2 radical in Comets C/1999 S4 (LINEAR) and C/2001 A2 (LINEAR). Following symmetry conservation laws, decay products maintain the spin distribution of the original molecules during photolysis, so that the OPR of NH_3 may be traced from that of NH_2. Kawakita et al. derived an OPR for NH_3 of 1.17 ± 0.04 and 1.12 ± 0.03, respectively, for the two LINEAR comets, corresponding to a spin temperature of ~30 K.

Several other cometary molecules (H_2CO, CH_3OH, hydrocarbons, …) are likely to have OPR effects that are worthy of investigation. The spin species of methane were found to be consistent with $T_{spin} > 40$–50 K (*Weaver et al.,* 1997; *Gibb et al.,* 2003). Formaldehyde was also investigated from its radio rotational lines, but no reliable OPR could be derived because only a few lines could be probed.

The cold spin temperatures retrieved for cometary H_2O and NH_3 presumably have a meaning related to the history of these species in the nucleus or even before, i.e., connected with their formation:

1. *Reequilibration in the nucleus.* We would then expect different spin temperatures for different comets, depending on their present orbit and dynamical history, which does not seem to be the case. 30 K corresponds to the equilibrium temperature at r ~ 100 AU, under present solar system conditions.

2. *Water formation.* The cold spin temperature would rule out a gas phase formation, since reactions leading to H_2O are exothermal and would form H_2O at a high temperature. Rather, the low OPR values suggest formation on grains, where H_2O would reequilibrate at the grain temperature (*Tielens and Allamandola,* 1987). The ortho-to-para conversion of H_2 on interstellar grains is very fast — on the order of 60 s. Thus, low OPR values are consistent with cometary H_2O originating in the interstellar medium.

3. *Fractionation of spin species.* It is also possible that one of the spin species is favored by condensation or absorption on interstellar or cometary grains, as is indeed observed in laboratory experiments such as condensation of D_2O on a cold matrix or selective absorption of H_2O on charcoal (*Tikhonov and Volkov,* 2002).

11. PERSPECTIVES

The situation regarding the detection and abundance determinations of cometary parent molecules has drastically changed since the publication of *Comets* (*Wilkening,* 1982). At that time, CO was the only parent molecule that had been directly identified. Generally, one had to rely on *deducing* the identity of the parents from observations of their daughter products. A half dozen species were proposed in these pioneering times, including H_2O, CO_2, CH_4, NH_3, all of which have been confirmed by recent observations.

We now have firm, direct identifications of two dozen parent molecules. It is very probable that the most abundant ones (say, at the level of ~1% relative to H_2O) are now known, including those already suggested 20 years ago. Many more molecules have emerged, some of them being only trace species (less than ~0.1%): other hydrocarbons, several nitriles and "CHO" species, and S-containing molecules.

Presumably, many additional molecules remain undetected in comets. The presence of unidentified lines (or blends of lines) strongly suggests that we are on the verge of important new discoveries. More molecules have been detected in the interstellar medium and even more in meteorites (e.g., *Botta and Bada,* 2002), with abundances generally decreasing with increasing complexity. No limit has yet been reached in the complexity of molecules found in these environments, and the same could be true for cometary material.

Future progress by remote sensing spectroscopy requires continual improvements in sensitivity, as is being provided now by new-generation instruments such as Keck/NIRSPEC, the Subaru telescope, and the Very Large Telescope, or planned intruments such as the Atacama Large Millimeter Array. Apparitions of new, bright comets are always highly anticipated, as they provide excellent opportunities to provide deeper searches than previously obtained. Short-period comets (and more specifically, Jupiter-family comets) are fainter objects, and therefore more difficult to study. Nevertheless, improvements in technology will hopefully allow investigations of parent molecules in a large fraction of the short-period comets. Laboratory work on molecular spectroscopy and the compilation of comprehensive spectroscopic databases are also needed for further progress.

An alternative approach is *in situ* analysis by space exploration, as will be performed by the *Rosetta* mission. Mass spectroscopy and gas chromatography could be much more sensitive than remote sensing.

Perhaps the ultimate answers regarding cometary composition will only be revealed by the analysis, at leisure on Earth, of returned samples of cometary ices. Unfortunately, there is not yet any approved space mission with this as its goal, but we can hope for such a mission in the not too distant future.

The cost and difficulty of encounter missions with comets will limit, probably for a long time, *in situ* investigations to a very small number of objects chosen among the short-period comets. Ground- and Earth-orbit-based observations will still be needed for the systematic investigation of a large sample of objects, in order to study their diversity. Only then will we truly be able to address the role that comets played in the formation and evolution of the solar system and their relation to the interstellar medium.

Acknowledgments. H.A.W. acknowledges financial support by NASA through grant HST-GO-8276.01-A from the Space Telescope Science Institute, which is operated by the Association of Universities for Research in Astronomy, Inc., under NASA Contract NAS5-26555, and through FUSE Grant NAG5-10921.

REFERENCES

A'Hearn M. F., Feldman P. D., and Schleicher D. J. (1983) The discovery of S_2 in comet IRAS-Araki-Alcock 1983d. *Astrophys. J. Lett., 274,* L99–L103.

A'Hearn M. F., Schleicher D. G., Millis R. L., Feldman P. D., and Thompson D. T. (1984) Comet Bowell 1980b. *Astron. J., 89,* 579–591.

A'Hearn M. F., Millis R. L., Schleicher D. G., Osip D. J., and Birch P. V. (1995) The ensemble properties of comets: Results from narrowband photometry of 85 comets, 1976–1992. *Icarus, 118,* 223–270.

Altenhoff W. J., Batrla W., Huchtmeier W. K., Schmidt J., Stumpff P., and Walmsley M. (1983) Radio observations of comet 1983d. *Astron. Astrophys., 125,* L19–L22.

Altwegg K. (1996) Sulfur in comet Halley. Habilitationsschrift, Univ. of Bern.

Altwegg K., Balsiger H., and Geiss J. (1994) Abundance and origin of the CH_n^+ ions in the coma of comet P/Halley. *Astron. Astrophys., 290,* 318–323.

Altwegg K., Balsiger H., and Geiss J. (1999) Composition of the volatile material in Halley's coma from in situ measurements. *Space Sci. Rev., 90,* 3–18.

Arpigny C., Jehin E., Manfroid J., Hutsemékers D., Schulz R., Stüve J. A., Zucconi J.-M., and Ilyin I. (2003) Anomalous nitrogen isotope ratio in comets. *Science, 301,* 1522–1524.

Ashihara O. (1975) The electron energy loss rates by polar molecules. *Inst. Space Aeronautical Sci. Rept. No. 530, 40,* 10.

Balsiger H., Altwegg K., and Geiss J. (1995) D/H and $^{18}O/^{16}O$ ratio in the hydronium ion and in neutral water from *in situ* ion measurements in comet P/Halley. *J. Geophys. Res., 100,* 5827–5834.

Bird M. K., Huchtmeier W. K., Gensheimer P., Wilson T. L., Janardhan P., and Lemme C. (1997) Radio detection of ammonia in comet Hale-Bopp. *Astron. Astrophys., 325,* L5–L8.

Bird M. K., Janardhan P., Wilson T. L., Huchtmeier W. K., Gensheimer P., and Lemme C. (1999) K-band radio observations of comet Hale-Bopp: Detections of ammonia and (possibly) water. *Earth Moon Planets, 78,* 21–28.

Bird M. K., Hatchell J., van der Tak F. F. S., Crovisier J., and Bockelée-Morvan D. (2002) Search for the radio lines of ammonia in comets. In *Proceedings of Asteroids Comets Meteors 2002* (B. Warmbein, ed.), pp. 697–700. ESA SP-500, Noordwijk, The Netherlands.

Biver N. and 22 colleagues (1997) Evolution of the outgassing of comet Hale-Bopp (C/1995 O1) from radio observations. *Science, 275,* 1915–1918.

Biver N. and 13 colleagues (1999a) Spectroscopic monitoring of comet C/1996 B2 (Hyakutake) with the JCMT and IRAM radio telescopes. *Astron. J., 118,* 1850–1872.

Biver N. and 22 colleagues (1999b) Long-term evolution of the outgassing of comet Hale-Bopp from radio observations. *Earth Moon Planets, 78,* 5–11.

Biver N. and 12 colleagues (2000) Spectroscopic observations of comet C/1999 H1 (Lee) with the SEST, JCMT, CSO, IRAM, and Nançay radio telescopes. *Astron. J., 120,* 1554–1570.

Biver N. and 23 colleagues (2002a) The 1995–2002 long-term monitoring of comet C/1995 O1 (Hale-Bopp) at radio wavelengths. *Earth Moon Planets, 90,* 5–14.

Biver N., Bockelée-Morvan D., Crovisier J., Colom P., Henry F., Moreno R., Paubert G., Despois D., and Lis D. C. (2002b) Chemical composition diversity among 24 comets observed at radio wavelengths. *Earth Moon Planets, 90,* 323–333.

Blake G. A., Qi C., Hogerheijde M. R., Gurwell M. A., and Muhleman D. O. (1999) Sublimation from icy jets as a probe of the interstellar content of comets. *Nature, 398,* 213–216.

Bockelée-Morvan D. (1987) A model for the excitation of water in comets. *Astron. Astrophys., 181,* 169–181.

Bockelée-Morvan D. (1997) Cometary volatiles. The status after comet C/1996 B2 (Hyakutake). In *Molecules in Astrophysics: Probes and Processes* (E. F. Van Dishoeck, ed.), pp. 219–255. IAU Symposium 178, Kluwer, Dordrecht.

Bockelée-Morvan D. and Crovisier J. (1985) Possible parents for the cometary CN radical: Photochemistry and excitation conditions. *Astron. Astrophys., 151,* 90–100.

Bockelée-Morvan D. and Crovisier J. (1989) The nature of the 2.8-μm emission feature in cometary spectra. *Astron. Astrophys., 216,* 278–283.

Bockelée-Morvan D. and Crovisier J. (1992) Formaldehyde in comets. II — Excitation of the rotational lines. *Astron. Astrophys., 264,* 282–291.

Bockelée-Morvan D., Crovisier J., Baudry A., Despois D., Perault M., Irvine W. M., Schloerb F. P., and Swade D. (1984) Hydrogen cyanide in comets — Excitation conditions and radio observations of comet IRAS-Araki-Alcock 1983d. *Astron. Astrophys., 141,* 411–418.

Bockelée-Morvan D., Colom P., Crovisier J., Despois D., and Paubert G. (1991) Microwave detection of hydrogen sulphide and methanol in Comet Austin (1989c1). *Nature, 350,* 318–320.

Bockelée-Morvan D., Crovisier J., Colom P., and Despois D. (1994) The rotational lines of methanol in comets Austin 1990 V and Levy 1990 XX. *Astron. Astrophys., 287,* 647–665.

Bockelée-Morvan D., Brooke T. Y., and Crovisier J. (1995) On the origins of the 3.2–3.6 μm emission feature in comets. *Icarus, 116,* 18–39.

Bockelée-Morvan D. and 11 colleagues (1998) Deuterated water in comet C/1996 B2 (Hyakutake) and its implications for the origin of comets. *Icarus, 133,* 147–162.

Bockelée-Morvan D. and 17 colleagues (2000) New molecules found in comet C/1995 O1 (Hale-Bopp). Investigating the link between cometary and interstellar material. *Astron. Astrophys., 353,* 1101–1114.

Bockelée-Morvan D. and 11 colleagues (2001) Outgassing behavior and composition of comet C/1999 S4 (LINEAR) during its disruption. *Science, 292,* 1339–1343.

Botta O. and Bada J. L. (2002) Extraterrestrial organic compounds in meteorites. *Survey Geophys., 23,* 411–467.

Brooke T. Y., Knacke R. F., Owen T. C., and Tokunaga A. T. (1989) Spectroscopy of emission features near 3 microns in Comet Wilson (1986l). *Astrophys. J., 336,* 971–978.

Brooke T. Y., Tokunaga A. T., Weaver H. A., Crovisier J., Bockelée-Morvan D., and Crisp D. (1996) Detection of acetylene in the infrared spectrum of comet Hyakutake. *Nature, 383,* 606–608.

Brooke T. Y., Weaver H. A., Chin G., Bockelée-Morvan D., Kim S. J., and Xu L.-H. (2003) Spectroscopy of comet Hale-Bopp in the infrared. *Icarus, 166,* 167–187.

Budzien S. A. and Feldman P. D. (1992) Upper limits to the S_2 abundance in several comets observed with the International Ultraviolet Explorer. *Icarus, 99,* 143–152.

Capria M. T., Coradini A., De Sanctis M. C., and Orosei R. (2000) CO emission mechanisms in C/1995 O1 (Hale-Bopp). *Astron. Astrophys., 357,* 359–366.

Chin G. and Weaver H. A. (1984) Vibrational and rotational excitation of CO in comets: nonequilibrium calculations. *Astrophys. J., 285,* 858–869.

Chiu K., Neufeld D. A., Bergin E. A., Melnick G. J, Patten B. M., Wang Z., and Bockelée-Morvan D. (2001) Post-perihelion SWAS observations of water vapor in the coma of comet C/1999 H1 (Lee). *Icarus, 154,* 345–349.

Clemett S. J., Maechling C. R., Zare R. N., Swan P. D., and Walker R. M. (1993) Identification of complex aromatic molecules in individual interplanetary dust particles. *Science, 262,* 721–725.

Cochran A. L. (2002) A search for N_2^+ in spectra of comet C/2002 C1 (Ikeya-Zhang). *Astrophys. J. Lett., 576,* L165–L168.

Cochran A. L., Cochran W. D., and Barker E. S. (2000) N_2^+ and CO^+ in comets 122P/1995 S1 (de Vico) and C/1995 O1 (Hale-Bopp). *Icarus, 146,* 583–593.

Colangeli L., Epifani E., Brucato R., Bussoletti E., De Sanctis C., Fulle M., Mennela V., Palomba E., Palumbo P., and Rotundi A. (1999) Infrared spectral observations of comet 103P/Hartley 2 by ISOPHOT. *Astron. Astrophys., 343,* L87–L90.

Colom P., Crovisier J., Bockelée-Morvan D., Despois D., and Paubert G. (1992) Formaldehyde in comets. I — Microwave observations of P/Brorsen-Metcalf (1989 X), Austin (1990 V) and Levy (1990 XX). *Astron. Astrophys., 264,* 270–281.

Combes M. and 16 colleagues (1988) The 2.5 to 12 μm spectrum of comet Halley from the IKS-VEGA experiment. *Icarus, 76,* 404–436.

Combi M. R., Harris W. R., and Smyth W.M. (2004) Gas dynamics and kinetics in the cometary coma: Theory and observations. In *Comets II* (M. C. Festou et al., eds.), this volume. Univ. of Arizona, Tucson.

Cottin H., Gazeau M.-C., Benilan Y., and Raulin F. (2004) Origin of cometary extended sources from degradation of refractory

organics on grains: Polyoxymethylene as formaldehyde parent molecule. *Icarus, 167,* 397–416.

Cravens T. E. and Korosmezey A. (1986) Vibrational and rotational cooling of electrons by water vapor. *Planet. Space Sci., 34,* 961–970.

Crifo J.-F., Fulle M., Kömle N. I., and Szegö K. (2004) Nucleus-coma structural relationships: Lessons from physical models. In *Comets II* (M. C. Festou et al., eds.), this volume. Univ. of Arizona, Tucson.

Crovisier J. (1984) The water molecule in comets: Fluorescence mechanisms and thermodynamics of the inner coma. *Astron. Astrophys., 130,* 361–372.

Crovisier J. (1987) Rotational and vibrational synthetic spectra of linear parent molecules in comets. *Astron. Astrophys. Suppl. Ser., 68,* 223–258.

Crovisier J. (1994) Photodestruction rates for cometary parent molecules. *J. Geophys. Res., 99,* 3777–3781.

Crovisier J. and Encrenaz T. (1983) Infrared fluorescence in comets: The general synthetic spectrum. *Astron. Astrophys., 126,* 170–182.

Crovisier J. and Le Bourlot J. (1983) Infrared and microwave fluorescence of carbon monoxide in comets. *Astron. Astrophys., 123,* 61–66.

Crovisier J., Despois D., Bockelée-Morvan D., Colom P., and Paubert G. (1991a) Microwave observations of hydrogen sulfide and searches for other sulfur compounds in comets Austin (1989c1) and Levy (1990c). *Icarus, 93,* 246–258.

Crovisier J., Encrenaz T., and Combes M. (1991b) Carbon suboxide in comet Halley. *Nature, 353,* 610.

Crovisier J., Leech K., Bockelée-Morvan D., Brooke T. Y., Hanner M. S., Altieri B., Keller H. U., and Lellouch E. (1997) The spectrum of Comet Hale-Bopp (C/1995 O1) observed with the Infrared Space Observatory at 2.9 AU from the Sun. *Science, 275,* 1904–1907.

Crovisier J., Leech K., Bockelée-Morvan D., Lellouch E., Brooke T. Y., Hanner M. S., Altieri B., Keller H. U., and Lim T. (1999a) The spectrum of comet Hale-Bopp as seen by ISO. In *The Universe as Seen by ISO* (P. Cox and M. F. Kessler, eds.), pp. 137–140. ESA SP-427, Noordwijk, The Netherlands.

Crovisier J. and 11 colleagues (1999b) ISO observations of short-period comets. In *The Universe as Seen by ISO* (P. Cox and M. F. Kessler, eds.), pp. 161–164. ESA SP-427, Noordwijk, The Netherlands.

Crovisier J., Bockelée-Morvan D., Colom P., Biver N., Despois D., Lis D. C., and the Team for Target-of-Opportunity Radio Observations of Comets (2004a) The composition of ices in comet C/1995 O1 (Hale-Bopp) from radio spectroscopy: Further results and upper limits on undetected species. *Astron. Astrophys., 418,* 1141–1157.

Crovisier J., Bockelée-Morvan D., Biver N., Colom P., Despois D., and Lis D. C. (2004b) Ethylene glycol in comet C/1995 O1 (Hale-Bopp). *Astron. Astrophys., 418,* L35–L38.

Davies J. K., Green S. F., and Geballe T. R. (1991) The detection of a strong 3.28 μm emission feature in comet Levy. *Mon. Not. R. Astron. Soc., 251,* 148–151.

Dello Russo N., DiSanti M. A., Mumma M. J., Magee-Sauer K., and Rettig T. W. (1998) Carbonyl sulfide in comets C/1996 B2 (Hyakutake) and C/1995 O1 (Hale-Bopp): Evidence for an extended source in Hale-Bopp. *Icarus, 135,* 377–388.

Dello Russo N., Mumma M. J., DiSanti M. A., Magee-Sauer K., Novak R., and Rettig T. W. (2000) Water production and release in Comet C/1995 O1 Hale-Bopp. *Icarus, 143,* 324–337.

Dello Russo N., Mumma M. J., DiSanti M. A., Magee-Sauer K., and Novak R. (2001) Ethane production and release in comet C/1995 O1 Hale-Bopp. *Icarus, 153,* 162–179.

Dello Russo N., Mumma M. J., DiSanti M. A., and Magee-Sauer K. (2002a) Production of ethane and water in comet C/1996 B2 Hyakutake. *J. Geophys. Res.–Planets, 107(E11),* 5095, doi:10.1029/2001JE001838.

Dello Russo N., DiSanti M. A., Magee-Sauer K., Gibb E., and Mumma M. J. (2002b) Production of C_2H_6 and H_2O in comet 2002 C1 Ikeya-Zhang on UT 2002 April 13.7–13.9. In *Proceedings of Asteroids Comets Meteors 2002* (B. Warmbein, ed.), pp. 689–692. ESA SP-500, Noordwijk, The Netherlands.

Dello Russo N., DiSanti M. A., Magee-Sauer K., Gibb E., Mumma M. J., Barber R. J., and Tennyson J. (2004) Water production and release in comet 153P/Ikeya-Zhang (2002 C1): Accurate rotational temperatures retrievals from hot-band lines near 2.9 μm. *Icarus, 168,* 186–200.

Despois D., Crovisier J., Bockelée-Morvan D., Schraml J., Forveille T., and Gérard E. (1986) Observation of hydrogen cyanide in comet Halley. *Astron. Astrophys., 160,* L11–L12.

DiSanti M. A., Mumma M. J., Dello Russo N., Magee-Sauer K., Novak R., and Rettig T. W. (1999) Identification of two sources of carbon monoxide in comet Hale-Bopp. *Nature, 399,* 662–665.

DiSanti M. A., Mumma M. J., Dello Russo N., and Magee-Sauer K. (2001) Carbon monoxide production and excitation in comet C/1995 O1 (Hale-Bopp): Isolation of native and distributed CO sources. *Icarus, 153,* 361–390.

DiSanti M. A., Dello Russo N., Magee-Sauer K., Gibb E. L., Reuter D. C., and Mumma M. J. (2002) CO, H_2CO and CH_3OH in comet 2002 C1 Ikeya-Zhang. In *Proceedings of Asteroids Comets Meteors 2002* (B. Warmbein, ed.), pp. 571–574. ESA SP-500, Noordwijk, The Netherlands.

DiSanti M. A., Mumma M. J., Dello Russo N., Magee-Sauer K., and Griep D. (2003) Evidence for a dominant native source of CO in comet C/1996 B2 (Hyakutake). *J. Geophys. Res., 108(E6),* 5061.

Dones L., Weissman P. R., Levison H. F., and Duncan M. J. (2004) Oort cloud formation and dynamics. In *Comets II* (M. C. Festou et al., eds.), this volume. Univ. of Arizona, Tucson.

Duncan M., Levison H., and Dones L. (2004) Dynamical evolution of ecliptic comets. In *Comets II* (M. C. Festou et al., eds.), this volume. Univ. of Arizona, Tucson.

Dutrey A. and 12 colleagues (1996) *Comet C/1996 B2 (Hyakutake).* IAU Circular No. 6364.

Eberhardt P. (1999) Comet Halley's gas composition and extended sources: Results from the neutral mass spectrometer on Giotto. *Space Sci. Rev., 90,* 45–52.

Eberhardt P. and 10 colleagues (1987) The CO and N_2 abundance in comet P/ Halley. *Astron. Astrophys., 187,* 481–484.

Eberhardt P., Meier R., Krankowsky D., and Hodges R. R. (1994) Methanol and hydrogen sulfide in comet P/Halley. *Astron. Astrophys., 288,* 315–329.

Eberhardt P., Reber M., Krankowsky D., and Hodges R. R. (1995) The D/H and $^{18}O/^{16}O$ ratios in water from comet P/Halley. *Astron. Astrophys., 302,* 301–316.

Ehrenfreund P., Charnley S. B., and Wooden D. (2004) From interstellar material to cometary particles and molecules. In *Comets II* (M. C. Festou et al., eds.), this volume. Univ. of Arizona, Tucson.

Feldman P. D. (1999) Ultraviolet observations of comet Hale-Bopp. *Earth Moon Planets, 79,* 145–160.

Feldman P. D. and Brune W. H. (1976) Carbon production in comet West (1975n). *Astrophys. J. Lett., 209,* L45–L48.

Feldman P. D. and 15 colleagues (1987) IUE observations of comet P/Halley: Evolution of the ultraviolet spectrum between September 1985 and July 1986. *Astron. Astrophys., 187,* 325–328.

Feldman P. D. and 14 colleagues (1991) Observations of Comet Levy (1990c) with the Hopkins Ultraviolet Telescope. *Astrophys. J. Lett., 379,* L37–L40.

Feldman P. D., Festou M. C., Tozzi G. P., and Weaver H. A. (1997) The CO_2/CO abundance ratio in 1P/Halley and several other comets observed by IUE and HST. *Astrophys. J., 475,* 829–834.

Feldman P. D., Weaver H. A., A'Hearn M. F., Festou M. C., McPhate J. B., and Tozzi G.-P. (1999) Ultraviolet imaging spectroscopy of comet Lee (C/1999 H1) with HST/STIS (abstract). *Bull. Am. Astron. Soc., 31,* 1127.

Feldman P. D., Weaver H. A., and Burgh E. B. (2002) Far Ultraviolet Spectroscopic Explorer observations of CO and H_2 emissions in comet C/2001 A2 (LINEAR). *Astrophys. J. Lett., 576,* L91–L94.

Feldman P. D., Cochran A. L., and Combi M. R. (2004) Spectroscopic investigations of fragment species in the coma. In *Comets II* (M. C. Festou et al., eds.), this volume. Univ. of Arizona, Tucson.

Festou M. C., Rickman H., and West R. M. (1993) Comets. I — Concepts and observations. *Astron. Astrophys. Rev., 4,* 363–447.

Geiss J., Altwegg K., Anders E., Balsiger H., Ip W.-H., Meier A., Neugebauer M., Rosenbauer H., and Shelley E. G. (1991) Interpretation of the ion mass per charge range 25–35 amu/e obtained in the inner coma of Halley's comet by the HIS-sensor of the Giotto IMS experiment. *Astron. Astrophys., 247,* 226–234.

Gibb E. L., Mumma M. J., Dello Russo N., DiSanti M. A., and Magee-Sauer K. (2003) Methane in Oort cloud comets. *Icarus, 165,* 391–406.

Green J. C., Cash W., Cook T. A., and Stern S. A. (1991) The spectrum of comet Austin from 910 to 1180 Å. *Science, 251,* 408–410.

Greenberg J. M. and Li A. (1998) From interstellar dust to comets: The extended CO source in comet Halley. *Astron. Astrophys., 332,* 374–384.

Gunnarsson M., Rickman H., Festou M. C., Winnberg A., and Tancredi G. (2002) An extended CO source around comet 29P/Schwassmann-Wachmann 1. *Icarus, 157,* 309–322.

Gunnarsson M. and 14 colleagues (2003) Production and kinematics of CO in comet C/1995 O1 (Hale-Bopp) at large post-perihelion distances. *Astron. Astrophys., 402,* 383–393.

Haser L. (1957) Distribution d'intensité dans la tête d'une comète. *Bull. Acad. R. Sci. Liège, 43,* 740–750.

Henry F. (2003) La comète Hale-Bopp à l'interféromètre du Plateau de Bure: Étude de la distribution du monoxyde de carbone. Thèse de Doctorat, Université de Paris 6.

Henry F., Bockelée-Morvan D., Crovisier J., and Wink J. (2002) Observations of rotating jets of carbon monoxide in comet Hale-Bopp with the Plateau de Bure interferometer. *Earth Moon Planets, 90,* 57–60.

Hirota T., Yamamoto S., Kawaguchi K., Sakamoto A., and Ukita N. (1999) Observations of HCN, HNC and NH_3 in comet Hale-Bopp. *Astrophys. J., 520,* 895–900.

Hoban S., Mumma M. J, Reuter D. C., DiSanti M. A., Joyce R. R., and Storrs A. (1991) A tentative identification of methanol as the progenitor of the 3.52-micron emission feature in several comets. *Icarus, 93,* 122–134.

Hoban S., Reuter D. C., DiSanti M. A., Mumma M. J, and Elston R. (1993) Infrared observations of methanol in comet P/Swift-Tuttle. *Icarus, 105,* 548–556.

Huebner W. F (1987) First polymer in space identified in Comet Halley. *Science, 237,* 628–630.

Huebner W. F., Keady J. J., and Lyon S. P. (1992) Solar photo rates for planetary atmospheres and atmospheric pollutants. *Astrophys. Space Sci., 195,* 1–289.

Huntress W. T. Jr., Allen M., and Delitsky M. (1991) Carbon suboxide in comet Halley? *Nature, 352,* 316–318.

Irvine W. and 17 colleagues (1996) Spectroscopic evidence for interstellar ices in Comet Hyakutake. *Nature, 382,* 418–420.

Irvine W. M., Bergin E. A., Dickens J. E., Jewitt D., Lovell A. J., Matthews H. E., Schloerb F. P., and Senay M. (1998) Chemical processing in the coma as the source of cometary HNC. *Nature, 393,* 547–550.

Irvine W. M., Schloerb F. P., Crovisier J., Fegley B., and Mumma M. J. (2000a) Comets: A link between interstellar and nebular chemistry. In *Protostars and Planets IV* (V. Mannings et al., eds.), pp. 1159–1200. Univ. of Arizona, Tucson.

Irvine W. M., Senay M., Lovell A. J., Matthews H. E., McGonagle D., and Meier R. (2000b) NOTE: Detection of nitrogen sulfide in comet Hale-Bopp. *Icarus, 143,* 412–414.

Irvine W. M., Bergman P., Lowe T. B., Matthews H., McGonagle D., Nummelin A., and Owen T. (2003) HCN and HNC in comets C/2000 WM1 (LINEAR) and C/2002 C1 (Ikeya-Zhang). *Origins Life Evol. Biosph., 33,* 1–11.

Itikawa Y. J. (1972) Rotational transition in an asymmetric-top molecule by electron collision: Applications to H_2O. *J. Phys. Soc. Japan, 32,* 217–226.

Jacquinet-Husson and 47 colleagues (1999) The 1997 spectroscopic GEISA databank. *J. Quant. Spectrosc. Radiat. Transfer, 62,* 205–254. Also available on line at http:// ara.lmd.polytechnique.fr.

Jewitt D. C., Matthews H. E., Owen T. C., and Meier R. (1997) Measurements of $^{12}C/^{13}C$, $^{14}N/^{15}N$, and $^{32}S/^{34}S$ ratios in comet Hale-Bopp (C/1995 O1). *Science, 278,* 90–93.

Joblin C., Boissel P., and de Parseval P. (1997) Polycyclic aromatic hydrocarbon lifetime in cometary environments. *Planet. Space Sci., 45,* 1539–1542.

Johnson J. R., Fink U., and Larson H. P. (1983) The 0.9–2.5 micron spectrum of Comet West 1976 VI. *Astrophys. J., 270,* 769–777.

Kawakita H. and 18 colleagues (2001) The spin temperature of NH_3 in comet C/1999 S4 (LINEAR). *Science, 294,* 1089–1091.

Kawakita H., Watanabe J., Fuse T., Furusho R., and Abe S. (2002) Spin temperature of ammonia determined from NH_2 in comet C/2001 A2 (LINEAR). *Earth Moon Planets, 90,* 371–379.

Kawakita H., Watanabe J., Kinoshita D., Ishiguro M., and Nakamura R. (2003) Saturated hydrocarbons in Comet 153P/Ikeya-Zhang: Ethane, methane, and monodeuterio-methane. *Astrophys. J., 590,* 573–578.

Kim S. J. and A'Hearn M. F. (1991) Upper limits of SO and SO_2 in comets. *Icarus, 90,* 79–95.

Kim S. J., A'Hearn M. F., Wellnitz D. D., Meier R., and Lee Y. S. (2003) The rotational stucture of the B-X system of sulfur dimers in the spectra of comet Hyakutake (C/1996 B2). *Icarus, 166,* 157–166.

Kleine M., Wyckoff S., Wehinger P. A., and Peterson B. A. (1995) The carbon isotope abundance ratio in comet Halley. *Astrophys. J., 439,* 1021–1033.

Knacke R. F., Brooke T. Y., and Joyce R. R. (1986) Observations of

3.2–3.6 micron emission features in comet Halley. *Astrophys. J. Lett., 310,* L49–L53.

Krankowsky D. and 18 colleagues (1986) In situ gas and ion measurements at comet Halley. *Nature, 321,* 326–329.

Krasnopolsky V. A. and Mumma M. J. (2001) Spectroscopy of Comet Hyakutake at 80–700 Å: First detection of solar wind charge transfer emissions. *Astrophys. J., 549,* 629–634.

Krasnopolsky V. A., Mumma M. J., Abbott M., Flynn B. C., Meech K. J., Yeomans D. K., Feldman P. D., and Cosmovici C. B. (1997) Detection of soft X-rays and a sensitive search for noble gases in comet Hale-Bopp (C/1995 O1). *Science, 277,* 1488–1491.

Larson L., Weaver H. A., Mumma M. J., and Drapatz S. (1989) Airborne infrared spectroscopy of comet Wilson (1986l) and comparisons with comet Halley. *Astrophys. J., 338,* 1106–1114.

Lecacheux A. and 21 colleagues (2003) Observations of water in comets with Odin. *Astron. Astrophys., 402,* L55–L58.

Lis D. C., Keene J., Young K., Phillips T. G., Bockelée-Morvan D., Crovisier J., Schilke P., Goldsmith P. F., and Bergin E. A. (1997) Spectroscopic observations of comet C/1996 B2 (Hyakutake) with the Caltech Submillimeter Observatory. *Icarus, 130,* 355–372.

Lis D. C. and 10 colleagues (1999) New molecular species in comet C/1995 O1 (Hale-Bopp) observed with the Caltech Submillimeter Observatory. *Earth Moon Planets, 78,* 13–20.

Lisse C. M., Cravens T. E., and Dennerl K. (2004) X-ray and extreme ultraviolet emission from comets. In *Comets II* (M. C. Festou et al., eds.), this volume. Univ. of Arizona, Tucson.

Lovell A. J. (1999) Millimeter-wave molecular mapping of comets Hyakutake and Hale-Bopp. PhD thesis, Univ. of Massachusetts.

Lunine J. I. and Gautier D. I. (2004) Coupled physical and chemical evolution of volatiles in the protoplanetary disk: A tale of three elements. In *Comets II* (M. C. Festou et al., eds.), this volume. Univ. of Arizona, Tucson.

Magee-Sauer K., Mumma M. J., DiSanti M. A., Dello Russo N., and Rettig T. W. (1999) Infrared spectroscopy of the ν_3 band of hydrogen cyanide in comet C/1995 O1 Hale-Bopp. *Icarus, 142,* 498–508.

Magee-Sauer K., Mumma M. J., DiSanti M. A., and Dello Russo N. (2002a) Hydrogen cyanide in comet C/1996 B2 Hyakutake. *J. Geophys. Res.–Planets, 107(E11),* 5096, doi:10.1029/2002JE001863.

Magee-Sauer K., Dello Russo N., DiSanti M. A., Gibb E., and Mumma M. J. (2002b) Production of HCN and C_2H_2 in comet C/2002 C1 (Ikeya-Zhang) on UT 2002 April 13.8. In *Proceedings of Asteroids Comets Meteors 2002* (B. Warmbein, ed.), pp. 549–552. ESA SP-500, Noordwijk, The Netherlands.

McPhate J. B., Feldman P. D., Weaver H. A., A'Hearn M. F., Tozzi G.-P., and Festou M. C. (1996) Ultraviolet CO emission in comet C/1996 B2 (Hyakutake) (abstract). *Bull. Am. Astron. Soc., 28,* 1093–1094.

Meech K. J. and Svoreň J. (2004) Physical and chemical evolution of cometary nuclei. In *Comets II* (M. C. Festou et al., eds.), this volume. Univ. of Arizona, Tucson.

Meier R. and A'Hearn M. F. (1997) Atomic sulfur in cometary comae based on UV spectra of the SI triplet near 1814 Å. *Icarus, 125,* 164–194.

Meier R., Eberhardt P., Krankowsky D., and Hodges R. R. (1993) The extended formaldehyde source in comet P/Halley. *Astron. Astrophys., 277,* 677–690.

Meier R., Eberhardt P., Krankowsky D., and Hodges R. R. (1994) Ammonia in comet P/Halley. *Astron. Astrophys., 287,* 268–278.

Meier R., Owen T. C., Matthews H. E., Jewitt D. C., Bockelée-Morvan D., Biver N., Crovisier J., and Gautier D. (1998a) A determination of the HDO/H_2O ratio in comet C/1995 O1 (Hale-Bopp). *Science, 279,* 842–844.

Meier R., Owen T. C., Jewitt D. C., Matthews H., Senay M., Biver N., Bockelée-Morvan D., Crovisier J., and Gautier D. (1998b) Deuterium in comet C/1995 O1 (Hale-Bopp): Detection of DCN. *Science, 279,* 1707–1710.

Meier R., Wellnitz D., Kim S. J., and A'Hearn M. F. (1998c) The NH and CH bands of comet C/1996 B2 (Hyakutake). *Icarus, 136,* 268–279.

Mitchell D. L., Lin R. P., Anderson K. A., Carlson C. W., Curtis D. W., Korth A., Reme H., Sauvaud J. A., d'Uston C., and Mendis D. A. (1987) Evidence for chain molecules enriched in carbon, hydrogen, and oxygen in comet Halley. *Science, 237,* 626–628.

Mitchell D. L., Lin R. P., Anderson K. A., Carlson C. W., Curtis D. W., Korth A., Reme H., Sauvaud J. A., d'Uston C., and Mendis D. A. (1989) Complex organic ions in the atmosphere of comet Halley. *Adv. Space Res., 9,* 35–39.

Morbidelli A. and Brown M. E. (2004) The Kuiper belt and the primordial evolution of the solar system. In *Comets II* (M. C. Festou et al., eds.), this volume. Univ. of Arizona, Tucson.

Moreels G., Clairemidi J., Hermine P., Brechignac P., and Rousselot P. (1993) Detection of a polycyclic aromatic molecule in P/Halley. *Astron. Astrophys., 282,* 643–656.

Müller H. S. P., Thorwirth S., Roth D. A., and Winnewisser G. (2001) The Cologne Database for Molecular Spectroscopy, CDMS. *Astron. Astrophys., 370,* L49–L52. Available on line at http://www.cdms.de.

Mumma M. J. (1982) Speculations on the infrared molecular spectra of comets. In *Vibrational-Rotational Spectroscopy for Planetary Atmospheres* (M. J. Mumma et al., eds.), pp. 717–742. NASA CP-2223, Vol. 2, Washington, DC.

Mumma M. J. and Reuter D. C. (1989) On the identification of formaldehyde in Halley's comet. *Astrophys. J., 344,* 940–948.

Mumma M. J., Stone E. J., and Zipf E. C. (1975) Nonthermal rotational distribution of CO ($A^1\Pi$) fragments produced by dissociative excitation of CO_2 by electron impact. *J. Geophys. Res., 80,* 161–167.

Mumma M. J., Weaver H. A., Larson H. P., Davis D. S., and Williams M. (1986) Detection of water vapor in Halley's comet. *Science, 232,* 1523–1528.

Mumma M. J., Weissman P. R., and Stern S. A. (1993) Comets and the origin of the solar system: Reading the Rosetta Stone. In *Protostars and Planets III* (E. H. Levy and J. I. Lunine, eds.), pp. 1177–1252. Univ. of Arizona, Tucson.

Mumma M. J., DiSanti M. A., Tokunaga A., and Roettger E. E. (1995) Ground-based detection of water in Comet Shoemaker-Levy 1992 XIX; probing cometary parent molecules by hot-band fluorescence (abstract). *Bull. Am. Astron. Soc., 27,* 1144.

Mumma M. J., DiSanti M. A., Dello Russo N., Fomenkova M., Magee-Sauer K., Kaminski C. D., and Xie D.X. (1996) Detection of abundant ethane and methane, along with carbon monoxide and water, in comet C/1996 B2 Hyakutake: Evidence for interstellar origin. *Science, 272,* 1310–1314.

Mumma M. J., DiSanti M. A., Dello Russo N., Magee-Sauer K., and Rettig T. W. (2000) Detection of CO and ethane in comet 21P/Giacobini-Zinner: Evidence for variable chemistry in the outer solar nebula. *Astrophys. J. Lett., 531,* L155–L159.

Mumma M. J., Dello Russo N., DiSanti M. A., Magee-Sauer K., Novak R. E., Brittain S., Rettig T., McLean I. S., Reuter D. C., and Xu L. (2001a) Organic composition of C/1999 S4 (LINEAR): A comet formed near Jupiter? *Science, 292,* 1334–1339.

Mumma M. J. and 18 colleagues (2001b) A survey of organic volatile species in comet C/1999 H1 (Lee) using NIRSPEC at the Keck Observatory. *Astrophys. J., 546,* 1183–1193.

Mumma M. J., DiSanti M. A., Dello Russo N., Magee-Sauer K., Gibb E., and Novak R. (2003) Remote infrared observations of parent volatiles in comets: A window on the early solar system. *Adv. Space Res., 31,* 2563–2575.

Neufeld D. A. and 19 colleagues (2000) SWAS observations of water towards comet C/1999 H1 (Lee). *Astrophys. J. Lett., 539,* L151–L154.

Palmer P., Wootten A., Butler B., Bockelée-Morvan D., Crovisier J., Despois D., and Yeomans D. K. (1996) Comet Hyakutake: First secure detection of ammonia in a comet (abstract). *Bull. Am. Astron. Soc., 28,* 927.

Pickett H. M., Poynter R. L., Cohen E. A., Delitsky M. L., Pearson J. C., and Müller H. S. P. (1998) Submillimeter, millimeter and microwave spectral line catalogue. *J. Quant. Spectrosc. Radiat. Transfer, 60,* 883–890. Available on line at http://spec.jpl.nasa.gov.

Prialnik D., Benkhoff J., and Podolak M. (2004) Modeling the structure and activity of comet nuclei. In *Comets II* (M. C. Festou et al., eds.), this volume. Univ. of Arizona, Tucson.

Rauer H. and 12 colleagues (2003) Long-term optical spectrophotometric monitoring of comet C/1995 O1 (Hale-Bopp). *Astron. Astrophys., 397,* 1109–1122.

Raymond J. C., Uzzo M., Ko Y.-K., Mancuso S., Wu R., Gardner L., Kohl J. L., Marsden B., and Smith P. L. (2002) Far-ultraviolet observations of Comet 2P/Encke at perihelion. *Astrophys. J., 564,* 1054–1060.

Reuter D. C., Hoban S., and Mumma M. J. (1992) An infrared search for formaldehyde in several comets. *Icarus, 95,* 329–332.

Reylé C. and Boice D. C. (2003) A S_2 fluorescence model for interpreting high resolution cometary spectra. I. Model description and initial results. *Astrophys. J., 587,* 464–471.

Rothman L. S. and 30 colleagues (2003) The HITRAN molecular spectroscopic database: Edition of 2000 including updates through 2001. *J. Quant. Spectrosc. Radiat. Transfer, 82,* 5–44. Available on line at http://www.hitran.com.

Schleicher D. G., Millis R. L., and Birch P. V. (1998) Narrowband photometry of comet P/Halley: Variation with heliocentric distance, season, and solar phase angle. *Icarus, 132,* 397–417.

Schloerb F. P., Kinzel W. M., Swade D. A., and Irvine W. M. (1986) HCN production rates from comet Halley. *Astrophys. J. Lett., 310,* L55–L60.

Schloerb F. P., Kinzel W. M., Swade D. A., and Irvine W. M. (1987) Observations of HCN in comet P/Halley. *Astron. Astrophys., 187,* 475–480.

Senay M. C. and Jewitt D. (1994) Coma formation driven by carbon monoxide release from comet Schwassmann-Wachmann 1. *Nature, 371,* 229–231.

Snyder L. E., Palmer P., and de Pater I. (1989) Radio detection of formaldehyde emission from Comet Halley. *Astrophys. J., 97,* 246–253.

Snyder L. E., Veal J. M., Woodney L. M., Wright M. C. H., Palmer P., A'Hearn M. F., Kuan Y.-J., de Pater I., and Forster J. R. (2001) BIMA array photodissociation measurements of HCN and CS in comet Hale-Bopp (C/1995 O1). *Astron. J., 121,* 1147–1154.

Stern S. A (2003) The evolution of comets in the Oort cloud and Kuiper belt. *Nature, 424,* 639–642.

Stern S. A., Green J. C., Cash W., and Cook T. A. (1992) Helium and argon abundance constraints and the thermal evolution of comet Austin (1989c1). *Icarus, 95,* 157–161.

Stern S. A., Slater D. C., Festou M. C., Parker J. W., Gladstone, G. R., A'Hearn M. F., and Wilkinson E. (2000) The discovery of argon in comet C/1995 O1 (Hale-Bopp). *Astrophys. J. Lett., 544,* L169–L172.

Swings P. (1941) Complex structure of cometary bands tentatively ascribed to the contour of the solar spectrum. *Lick Obs. Bull., 508,* 131–136.

Tielens A. G. G. M. and Allamandola L. J. (1987) Composition, structure, and chemistry of interstellar dust. In *Interstellar Processes* (D. J. Hollenbach and H. A. Thronson Jr., eds.), pp. 397–469. Reidel, Dordrecht.

Tikhonov V. I. and Volkov A. A. (2002) Separation of water into its ortho and para isomers. *Science, 296,* 2363.

Tokunaga A. T., Nagata T., and Smith R. G. (1987) Detection of a new emission band at 2.8 microns in comet P/Halley. *Astron. Astrophys., 187,* 519–522.

Tozzi G. P., Feldman P. D., and Festou M. C. (1998) Origin and production of C(^{1}D) atoms in cometary comae. *Astron. Astrophys., 330,* 753–763.

Veal J. M, Snyder L. E., Wright M., Woodney L. M., Palmer P., Forster J. R., de Pater I., A'Hearn M. F., and Kuan Y.-J. (2000) An interferometric study of HCN in comet Hale-Bopp (C/1995 O1). *Astron. J., 119,* 1498–1511.

Weaver H. A. (1998) Comets. In *The Scientific Impact of the Goddard High Resolution Spectrograph (GHRS)* (J. C. Brandt et al., eds.), pp. 213–226. ASP Conference Series 143, Astronomical Society of the Pacific, San Francisco.

Weaver H. A. (2000) *Comet C/1999 S4 (LINEAR).* IAU Circular No. 7461.

Weaver H. A. and Mumma M. J. (1984) Infrared molecular emissions from comets. *Astrophys. J., 276,* 782–797. (Erratum: *Astrophys. J., 285,* 272.)

Weaver H. A., Mumma M. J., Larson H. P., and Davis D. S. (1986) Post-perihelion observations of water in comet Halley. *Nature, 324,* 441–446.

Weaver H. A., Feldman P. D., McPhate J. B., A'Hearn M. F., Arpigny C., and Smith T. E. (1994) Detection of CO Cameron band emission in comet P/Hartley 2 (1991 XV) with the Hubble Space Telescope. *Astrophys. J., 422,* 374–380.

Weaver H. A. and 11 colleagues (1996) *Comet C/1996 B2 (Hyakutake).* IAU Circular No. 6374.

Weaver H. A., Brooke T. Y., DiSanti M. A., Mumma M. J., Tokunaga A., Chin G., A'Hearn M. F., Owen T. C., and Lisse C. M. (1997) The methane abundance in comet C/1996 B2 (Hyakutake) (abstract). *Bull. Am. Astron. Soc., 29,* 1041.

Weaver H. A., Chin G., Bockelée-Morvan D., Crovisier J., Brooke T. Y., Cruikshank D. P., Geballe T. R., Kim S. J., and Meier R. (1999a) An infrared investigation of volatiles in comet 21P/Giacobini-Zinner. *Icarus, 142,* 482–497.

Weaver H. A., Brooke T. Y., Chin G., Kim S. J., Bockelée-Morvan D., and Davies J. K. (1999b) Infrared spectroscopy of comet Hale-Bopp. *Earth Moon Planets, 78,* 71–80.

Weaver H. A. and 20 colleagues (2001) HST and VLT investigations of the fragments of comet C/1999 S4 (LINEAR). *Science, 292,* 1329–1334.

Weaver H. A., Feldman P. D., Combi M. R., Krasnopolsky V., Lisse C. A., and Shemansky D. E. (2002a) A search for argon

and O VI in three comets using the Far Ultraviolet Spectroscopic Explorer. *Astrophys. J. Lett., 576,* L95–L98.

Weaver H. A., Feldman P. D., A'Hearn M. F., Arpigny C., Combi M. R., Festou M. C., and Tozzi G.-P. (2002b) Spatially-resolved spectroscopy of C/2002 C1 (Ikeya-Zhang) with HST (abstract). *Bull. Am. Astron. Soc., 34,* 853–854.

Wilkening L., ed. (1982) *Comets*. Univ. of Arizona, Tucson. 766 pp.

Wink J., Bockelée-Morvan D., Despois D., Colom P., Biver N., Crovisier J., Lellouch E., Davies J. K., Dent W. R. F., and Jorda L. (1999) Evidence for extended sources and temporal modulations in molecular observations of C/1995 O1 (Hale-Bopp) at the IRAM interferometer (abstract). *Earth Moon Planets, 78,* 63.

Winnberg A., Ekelund E., and Ekelund A. (1987) Detection of HCN in comet P/Halley. *Astron. Astrophys., 172,* 335–341.

Womack M., Festou M. C., and Stern A. A. (1997) The heliocentric evolution of key species in the distantly-active comet C/1995 O1 (Hale-Bopp). *Astron. J., 114,* 2789–2795.

Woodney L. M. (2000) Chemistry in comets Hyakutake and Hale-Bopp. Ph.D. thesis, Univ. of Maryland.

Woodney L., McMullin J., and A'Hearn M. F. (1997) Detection of OCS in comet Hyakutake (C/1996 B2) *Planet. Space Sci., 45,* 717–719.

Woodney L. M., A'Hearn M. F., McMullin J., and Samarasinha N. (1999) Sulfur chemistry at millimeter wavelengths in C/Hale-Bopp. *Earth Moon Planets, 78,* 69–70.

Woodney L. and 14 colleagues (2002) Morphology of HCN and CN in comet Hale-Bopp (1995 O1). *Icarus, 157,* 193–204.

Wright M.C.H. and 10 colleagues (1998) Mosaicked images and spectra of $J = 1 \rightarrow 0$ HCN and HCO^+ emission from comet Hale-Bopp (1995 O1). *Astron. J., 116,* 3018–3028.

Wyckoff S. W., Tegler S. C., and Engel L. (1991) Nitrogen abundance in comet Halley. *Astrophys. J., 367,* 641–648.

Wyckoff S., Kleine M., Peterson B. A., Wehinger P. A., and Ziurys L. M. (2000) Carbon isotope abundances in comets. *Astrophys. J., 535,* 991–999.

Xie X. and Mumma M. J. (1992) The effect of electron collisions on rotational populations of cometary water. *Astrophys. J., 386,* 720–728.

Yamamoto T. (1982) Evaluation of infrared line emission from constituent molecules of cometary nuclei. *Astron. Astrophys., 109,* 326–330.

Ziurys L. M., Savage C., Brewster M. A., Apponi A. J., Pesch T. C., and Wyckoff S. (1999) Cyanide chemistry in comet Hale-Bopp (C/1995 O1). *Astrophys. J. Lett., 527,* L67–L71.